Calibration Report of the **STAFF** Measurements in the Cluster Active Archive (CAA)

Prepared by

P. Robert, C. Burlaud and M. Maksimovic

Version 3.0
Updated by N. Cornilleau-Wehrlin, P. Robert and R. Piberne

Version 4.0
Updated By R. Piberne and P. Robert

Version 4.1
Updated By N. Cornilleau-Wehrlin, P. Canu and R. Piberne

Version 4.2
Updated By N. Cornilleau-Wehrlin, P. Canu, R. Piberne and R.Katra.

Content

1. Introduction

In the first part, this document briefly describes the STAFF experiment, the calibration method used, and the delivered products.

In the second part, a large number of cross-calibration studies are given, especially those with FGM, and summarizes the efforts done on this subject the past few years. The measurements by two common STAFF-SC and STAFF-SA frequency bands are also compared.

The cross-calibration results presented here are based on the talks given between the first cross-calibration workshop in ESTEC in February 2006 and the 19th CAA Cross-Calibration meeting, in Frascati, 2-4 April 2014.

Most of the studies presented here are developed in the article **CLUSTER STAFF search coils magnetometer calibration – comparisons with FGM** [12].

Both old and new results are summarized here.

A number of authors have been involved in this work, including P. Robert, N. Cornilleau-Wehrlin, C. Burlaud, M. Maksimovic, L. Mirioni, V. Bouzid, R. Piberne, P. Canu, Y. De Conchy, C. Lacombe, B. Grison, O. Santolik, O. Alexandrova and D. Attié.

2. Instrument Description

The CLUSTER STAFF experiment comprises a tri-axial search coils magnetic sensor (0.1 Hz – 4 kHz frequency range) and two on-board wave analyzers, a magnetic waveform unit (STAFF-SC) and a wave spectrum analyzers (STAFF-SA) that calculates the complete matrix for the 3xB + 2xE components; the electric waveform data are received from the EFW sensors. For more detail of the experiment, see references [1-2]. For information on the coordinate system used, see Appendix A: Coordinate systems used by STAFF definitions

2.1 STAFF–SC

- The magnetic waveform unit delivers 3 waveforms (B_x, B_y, B_z) from the pre-amplifier filtered in either of the two low-pass bandwidths, 0.1 - 10 Hz (Normal Bit Rate: NBR) and 0.1 - 180 Hz (High Bit Rate: HBR). Sampling rates are 25 and 450 Hz, respectively.

- The filtered signals are digitized by three 16 bits sampling and hold devices synchronized by DWP and sent to the DWP experiment.

- The A/D converters are the same for STAFF and EFW and synchronized by DWP in order to facilitate further combined wave analysis. The low pass filters are identical too.

- Due to the telemetry limitation, a compression from 16 to 12 bits is performed inside DWP for STAFF wave form data.

- The coordinate system of the level 1 (L1) data is the Spinning Sensor System (SSS, STAFF Sensor Reference Frame); this is a spinning frame. x and y axis are parallel to the EFW axis and z is parallel to the spacecraft spin axis.

- Level 2 data are given in GSE and in ISR2.

2.2 STAFF–SA

- The spectrum analyzer is designed to calculate the complete cross spectral matrix for the 5 available components, 3xB + 2xE, in the 8 Hz-4 kHz frequency range. The electric field components come from the EFW sensors.

- The analysis band is divided into 3 logarithmically distributed frequency sub-bands of 9 frequencies each.

- For each sub-band there are 3 automatic gain control (AGC): one for Bx channel (parallel to the spacecraft spin axis) and one for each couple of spinning components (B_y, B_z and E_y, E_z respectively). Note that here, x,y,z correspond to the Body Build coordinate system, where x is the spin axis. In this document, general convention for science data set z as the spin axis.

- The different modes are the combination of 3 parameters: the time resolution, the number of frequencies computed (2 or 3 bands), the number of wave components considered.

- The coordinate system used for the delivery products is the ISR2 (inverse of SR2, close to GSE).

3. Measurement Calibration Procedures

3.1 Calibrations procedures

This term overlaps different aspects:

- The calibration methods used to transform L1 data (waveform or spectra) into level 2 (L2) calibrated data.

The corresponding software (see [3] and [4]), that take for input L1 data files and calibration files, and produce L2 data files.

- The calibration files take into account the whole transfer function, including the sensors, the pre-amplifiers and eventually the filters. These files can be regularly updated by the exploitation of calibrated signals recorded during the on board calibration mode executed once per orbit and stored in the L1 data files. Up to now, the use of these calibrated signals has allowed to verify that the STAFF experiment performances have not changed since the commissioning phase. Nevertheless a more refined cross calibration study has shown the need to validate the on-ground calibration performed before launch. A detail study of the ground equipment together with detailed cross calibrations has allowed to valid new transfer functions. As it will be shown, the correction factor is about 10 % for frequencies less than 8 Hz for SC1 with respect to the 3 other spacecraft. Another 10% correction is to be applied to the whole frequency range to the 4 S/C transfer functions.

3.2 Cross–calibration procedures

There are several possibilities for cross-calibration activities:

- The STAFF-SC NBR mode delivers magnetic waveform up to 10 Hz. So, comparison with FGM data can be done at two levels:
    - The Doppler effect due to the STAFF sensor rotation into the DC magnetic field provides a strong sine signal in the spin plane. On this strong sine signal are superimposed the very low amplitude magnetic fluctuations. Once the sine signal is extracted, its amplitude and phase are determined and corrected by the transfer function. These X and Y calibrated components of the DC magnetic field in the spin plane can be directly compared with FGM data.
    - The 3 STAFF-SC calibrated waveforms, from about spin frequency (0.25 Hz) up to 10 Hz, can be compared to the FGM high resolution waveform in any coordinate system.
    - To check a possible dependency with frequency, the corresponding spectra can be also compared. This provides additional information on each instrument, sensitivity versus frequency.

- The STAFF-SC HBR mode delivers magnetic waveform up to 180 Hz, and so permits an overlap with the low part of the STAFF-SA frequency range (usually 64 Hz-4 kHz in HBR, but some dedicated mode may allow a comparison from 8 Hz). Thus, the spectra level and the spectra continuity of the two sub-experiments can be checked.

- For STAFF-SA, in addition to the cross-calibration mentioned above, it is possible to check the spectral continuity of the magnetic fluctuations with:
    - WBD (between 25 Hz and 4 kHz)

- The spectral continuity of the electric fluctuations with EFW in the same conditions as for the magnetic components as described above for STAFF-SC and STAFF-SA.
- WHISPER (between 2 kHz and 4 kHz)

4. Measurement Processing Procedures

4.1 Cleaning waveform procedures

As explained in 3.2, the Doppler effect due to the STAFF sensor rotation into the DC magnetic field provides a strong sine signal on the components perpendicular to the spin axis (X and Y). This sine amplitude is equal to the perpendicular DC magnetic field (from a few nT up to 2000 nT, value above which the STAFF signal saturates). On this strong sine signal are superimposed the very low amplitude magnetic fluctuations (~a few nT or less).

First, before the FFT procedure, it is necessary to remove this strong sine signal. Then, the FFT will be applied on the remaining useful signal. This process consists of fitting the signal with a pure sine signal, whose frequency is known (the spin frequency). The dedicated process, based on a harmonic analysis applied on a single spectral component, provides the fitted sine signal amplitude and phase. Note that those two parameters are useful for FGM DC field comparison. Finally, this pure sine signal is subtracted from the original one to retrieve the fluctuations. This process is very efficient in terms of rejection performance and CPU time. But it requires at least a minimum duration of two spin periods, where the DC field is supposed to be constant. For long-time windows, only a DC field average value is subtracted, and so the efficiency of the rejection is decreased. In any case, all frequencies are preserved, but the spin frequency. As we can see, one has to choose the best compromise between a not too short and a not too long window duration.

4.2 Classical calibration method for STAFF–SC

This method operates in up to 5 steps depending on the desired final product, steps that are given below:

4.2.1 Get Level 1 waveform (in Volts) as a series of successive windows.

→ Selecting window time length (Δt) determines the frequency resolution (Δf) as Δt.Δf =1. → TM count [0-65535] to Volt [-5V, +5 V].conversion.

—►Calibration step # **1**: Volts, spinning sensor system, with DC field.

4.2.2 "Cleaning" raw waveforms in the Spinning Sensor System (SSS).

→ Remove the spin tone signal (~ 1 nT up to ~ 5600 nT) high compared to the useful signal (~1 nT or less). This is done using a specific harmonic analysis process. There are then 2 data sets, waveform in TM volts without DC components and DC components XY

kept for further use. Those XY spin plane components are calibrated for step 5 processing and future FGM comparisons.

—►Calibration step # **2**: Volts, spinning sensor system, without DC field.

4.2.3 Calibration of each component in a given window.

→ *Signal Centering, trapezoidal windowing, FFT, complex transfer function including conversion from Volt to nT, correction by *1/G(f),*

- ➔ *At this step one gets the complex calibrated spectra in the spacecraft spinning reference frame*
- ➔ *To go back to time domain :cutoff at low frequency*
  - *0.1 Hz for further transformation into SR2/ISR2 reference frame,*
  - *0.6 Hz for further transformation into GSE*

Then apply an FFT^{-1}.

—►Calibration step # **3**: nTesla, spinning sensor system, without DC field.

4.2.4 Get calibrated time series data in nT, in a fixed reference frame.

→ *Apply the appropriate matrix, but it requires accurate spin phase computation from the Sun pulse.*

→depending on the desired reference frame, use the data set produced after either one of the filtering (see above)

—►Calibration step # **4**: nTesla, fixed SR2 system, without DC field, [Fmin,Fmax]. → *Change coordinate system possibility from SR2 to GSE, or other (GSM, MAG, GEO…) with RCL & Rocotlib software (see [4], [5], [6]). ISR2 is inverse SR2 opposite sense for z axis)*

4.2.5 Add DC field values on X and Y

—►Calibration step # **5**: nTesla, fixed SR2 system, with previous calibrated X-Y DC field.

This permits to compare STAFF and FGM spin plane components data.

The DC field is not added on the Z axis since it is very weak and not significant, due to the very low difference (below 0.5°) between the Z and spin axis.

Note that this method is well adapted to compute calibrated spectra, but does not allow getting a continuous calibrated waveform, because edges of calibration window are disturbed by the weighting function. The continuous calibration method has thus been developed and applied(see 4.3), after that satisfactory preliminary results had been obtained and presented at the *10th CAA Cross-Calibration meeting, Paris, 2-4 November 2009.*

The full processing line of STAFF data and output products is given in the next section.

4.3 CLUSTER STAFF–SC continuous calibration method for CWF.

The method described hereafter replaces the classical method to produce calibrated wave form data. Indeed, the classical method is well adapted to produce calibrated spectra, but does not deliver a continuous waveform. As a Fourier transform is applied on successive windows,

the calibrated signal is affected by edge effects. Various test has been done to check the validity of this method with respect to the classical one (see *10th CAA Cross-Calibration meeting, Paris, 2-4 November 2009* and 11th *CAA Cross-Calibration meeting, Goslar, 7-9 April 2010*).

The continuous calibration method is based on the classical method. Data are processed as a series of successive windows but now spaced by one or a few TM count (at 25 or 450 Hz), that implies an overlapping of 2 successive windows. Then a Gaussian windowing is applied, and only the central point (or a few central points), corresponding to the Gaussian maximum, are kept. The next window is taken by a time shift of only one (or a few) TM count.

The diagram hereafter summarizes this method:

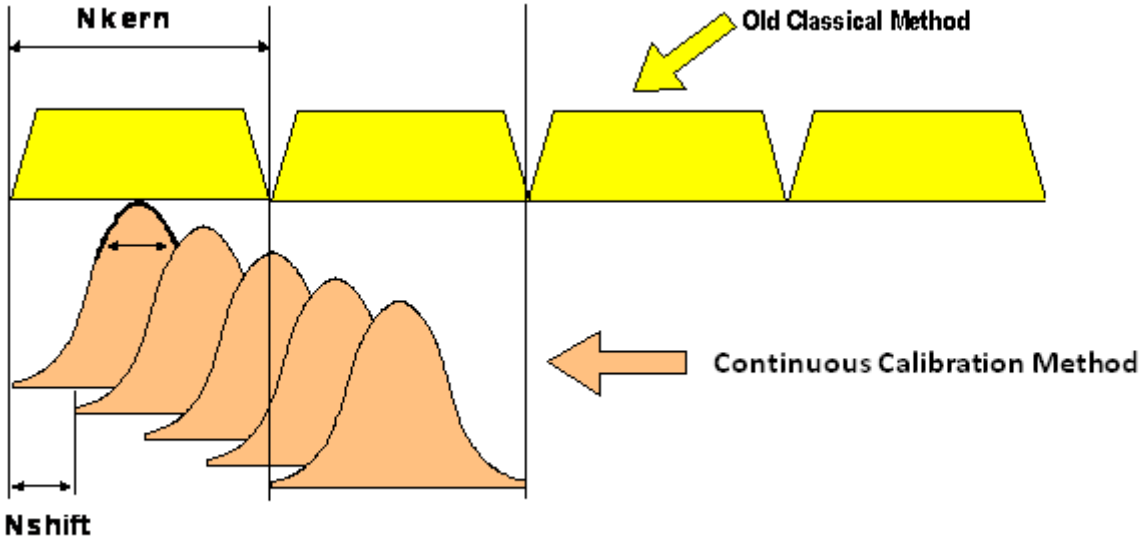

Figure 1: The schematic drawing of the two methods used for the production of continuous waveforms.

This method avoids the discontinuity on each window edge and a continuous calibrated waveform is also obtained. Nevertheless, it requires much CPU time.

Nkern must be chosen to - do a correct despin (> 2Ts, but not too long, ex: 512 points)
- have a high enough frequency resolution (not too short)

Nshift can be - the shortest possible (ex : 2 pts)
- could be extended to reduce CPU time without damage for the calibration quality (could be 6-8 pts)

The parameters chosen for NBR data are: Nkern = 1024, Nshift = 2

Note 1: In a first approach, the classical method has already been improved by a more efficient despin, (and so a better calibration), which is used in the continuous method. In particular, the phase continuity of the spin signal has been imposed.

Note 2: This method, working in the frequency domain, is comparable to the one chosen for Themis SCM data, where we remain in the time domain, and perform a convolution between the signal and the inverse of the impulse response of the transfer function. This is the same thing in term of mathematical approach, but different in term of coding. The choice of the frequency domain enables a more straightforward coding, and benefit of pieces of code already existing.

4.4 Full processing line

The logical flow diagram hereafter describes the full processing from the raw data until the level3 (L3) products.

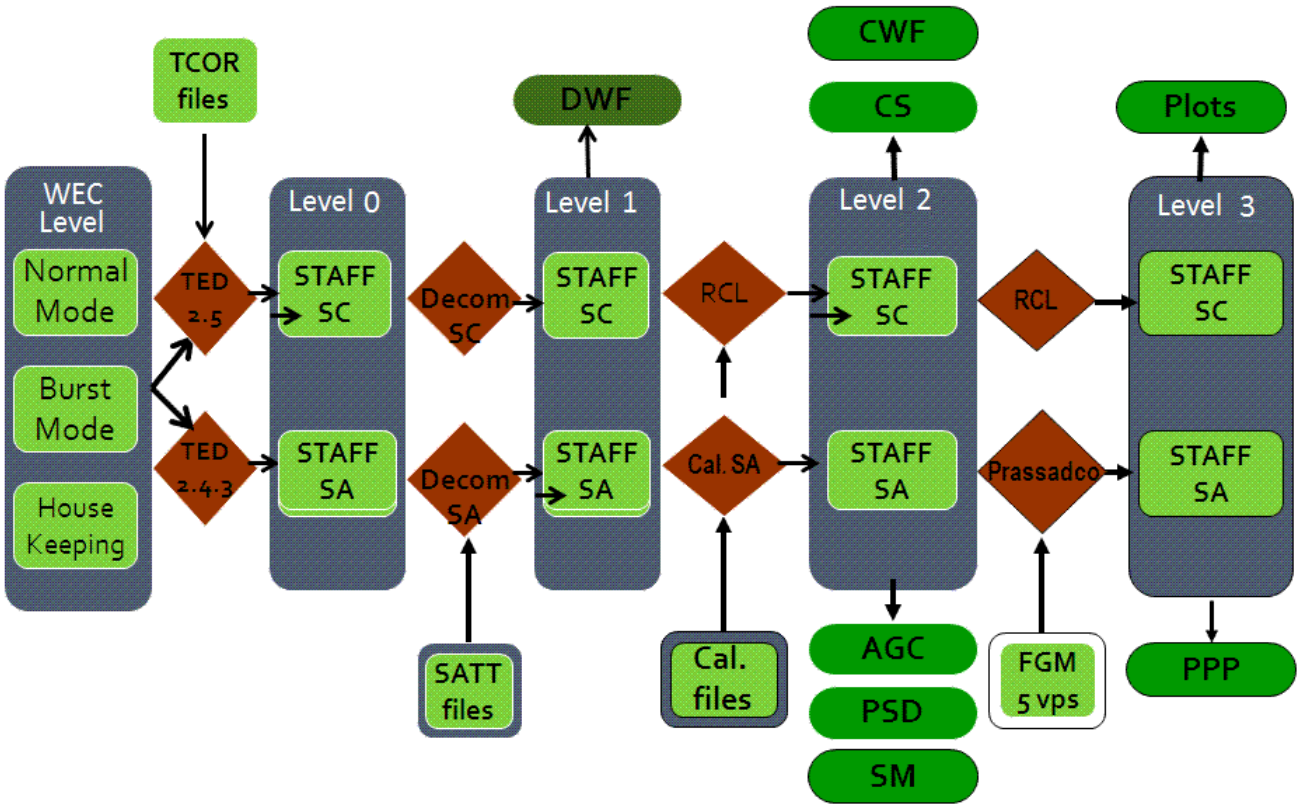

Figure 2: Processing chain for the data production.
The data products in green are delivered to the CAA.

Remarks:

- The TED software version used to process timestamping is different for STAFF-SC and STAFF-SA. For details, see UG or ICD.

- The STAFF-SC L1 data files, also called Decommutated Waveforms (DWF) are delivered to CAA because it is the only data pack containing all initial data (information about block data format, timestamps, compression quality, etc.), before any transformation such as calibration or change of reference frame.

- STAFF-SA calibration is done by dedicated software [7].

- STAFF-SC calibration is done using a part of RCL software (see [4]). RCL (Roproc Command Language) is a set of commands allowing many different data processes required for spatial experiment. This is an overcoat of the Roproc software (P. Robert's procedures, see [3]), initially developed for CLUSTER. RCL software allows the processing of CLUSTER data as well as data issued from any project/experiment, on any platform and Operating system (tested on SUN/Solaris, Linux, windows).

- The L2 to L3 processing is done by RCL for STAFF-SC and PRASSADCO for STAFF-SA (see [4 & 8]).

5. Results of Calibration Activities

There has been a problem on the calibration of STAFF-SC data for S/C #1.

- Problem identified after launch: the perpendicular DC-field measured by the spinning spacecraft at the spin frequency is not the same from S/C #1 than the other S/C: Difference is ~ 10 %. For an example, see the left panel of Figure 6: Comparisons of the modulus of the DC field in the plane perpendicular to the spin axis..

- S/C# 1 gives always lower values than other S/C for the DC field estimation from the spin signal.

- This difference is confirmed by FGM data.

This discrepancy has been identified thanks to coming back to old files of ground measurements of the transfer function: the current loop used was not the same as for other spacecraft and has been shown to have different characteristics. This has been shown to affect only the frequency range below 8 Hz. This is solved now by using for SC1 a transfer function that is the mean of the transfer functions of the 3 other spacecraft. The results are shown in section 6.

As will be seen in the description of the cross calibration activities, apart from SC1, when comparing SC2, 3 and 4 DC field and waveform in NBR (f< 10 Hz) with FGM, an additional difference of about 10 % was evidenced. This point together with the issue on SC1 led to a review of the ground equipment.
The above differences have been understood and the transfer functions updated accordingly.

Main conclusions are given in section 6.

6. Consequences of multiple irregular data gaps

The calibration methods used for CWF and CS as described in 4.3 rely on continuous times series of DWF. During period of poor spacecraft telemetry (hatched telemetry) and then discontinuous time series, there will be missing CWF and CS which will extend beyond the period of the missing points, with missing data periods different between these 2 data sets because of the different calibration methods and parameters used.

As explained in 4.3, CWF are calibrated using “continuous calibration” while CS are calibrated with the old “calibration method”. The parameters that were chosen in order to see the maximum of events are the following:

- For CWF:
  - NBR default window : 1024 pts
  - HBR default window : 4096 pts

  Calibration window shift = 2 points (default).

- For CS:
  - NBR default window : 256 pts
  - HBR default window : 4096 pts

  The window is entirely shifted.

We see that the parameters are not the same in NBR mode. This non-homogeneous situation may lead to produce CS and not CWF when the telemetry is hatched, depending on the time delay between missing points.
Indeed, in NBR mode, if one point is missing in DWF, it will result that the 511 previous and 511 next points can’t be calibrated in CWF while only the current window of 256 points can’t be calibrated in CS. So, if we have consecutive windows of 1024 points with only one point missing in each of these windows, there will be no CWF data produced at all while CS data will contain 2 to 3 calibrated spectra points in each of these windows.

Here is an example:

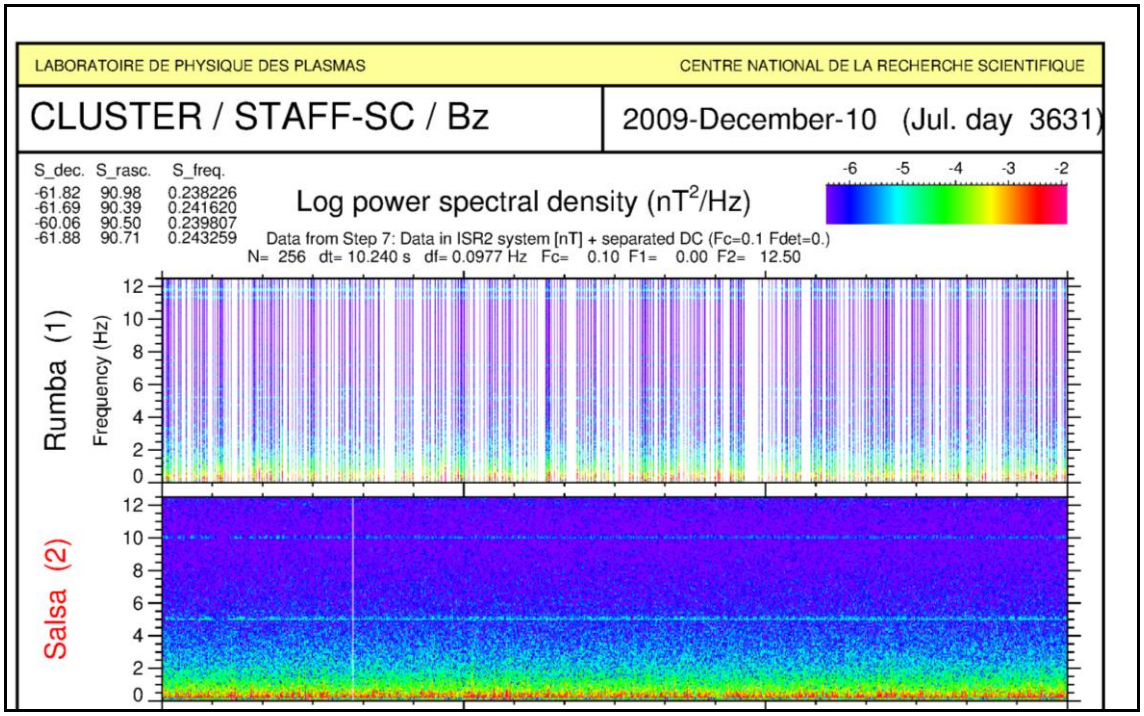

Figure 3: Example of CS data obtained with hatched telemetry in NBR mode

We can see that despite the lack of data, the PSD seen by C1 is pretty similar to the PSD seen by C2. For this day, no CWF are produced for C1.

We can note that such cases will only appear in NBR mode, due to the in-homogenous choice of the calibration window.

Figure 4 and Figure 5 show the same day in NBR and HBR mode.

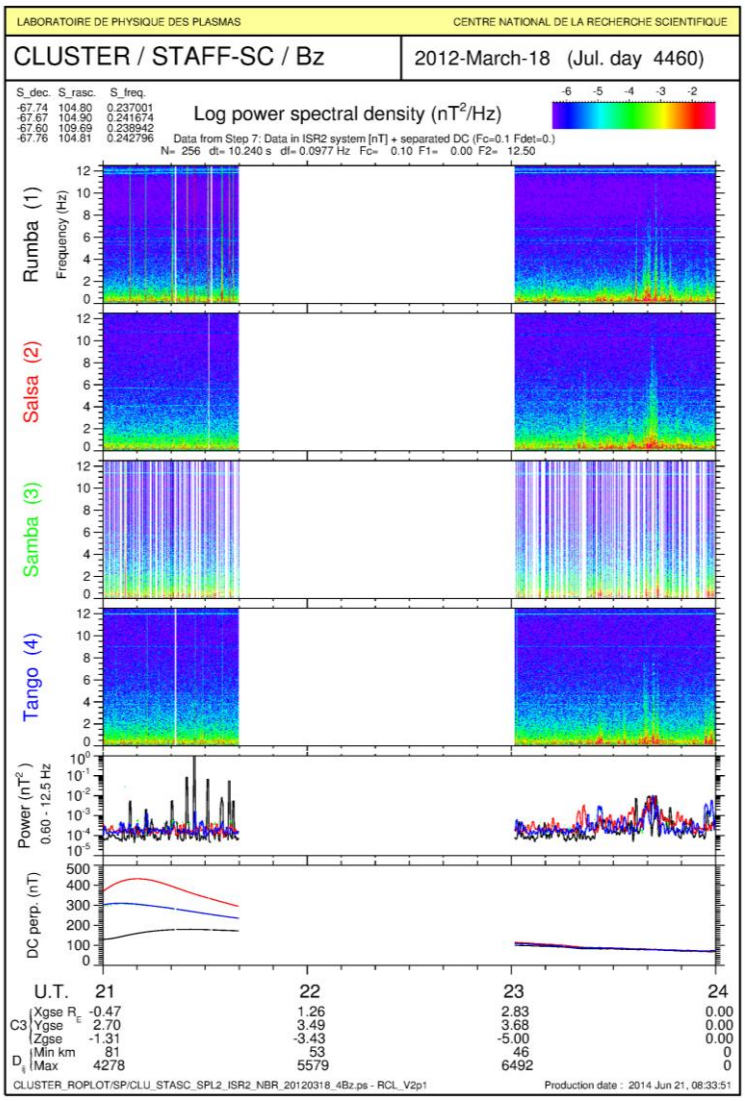

Figure 4: 2nd example of CS data obtained with hatched telemetry in NBR mode

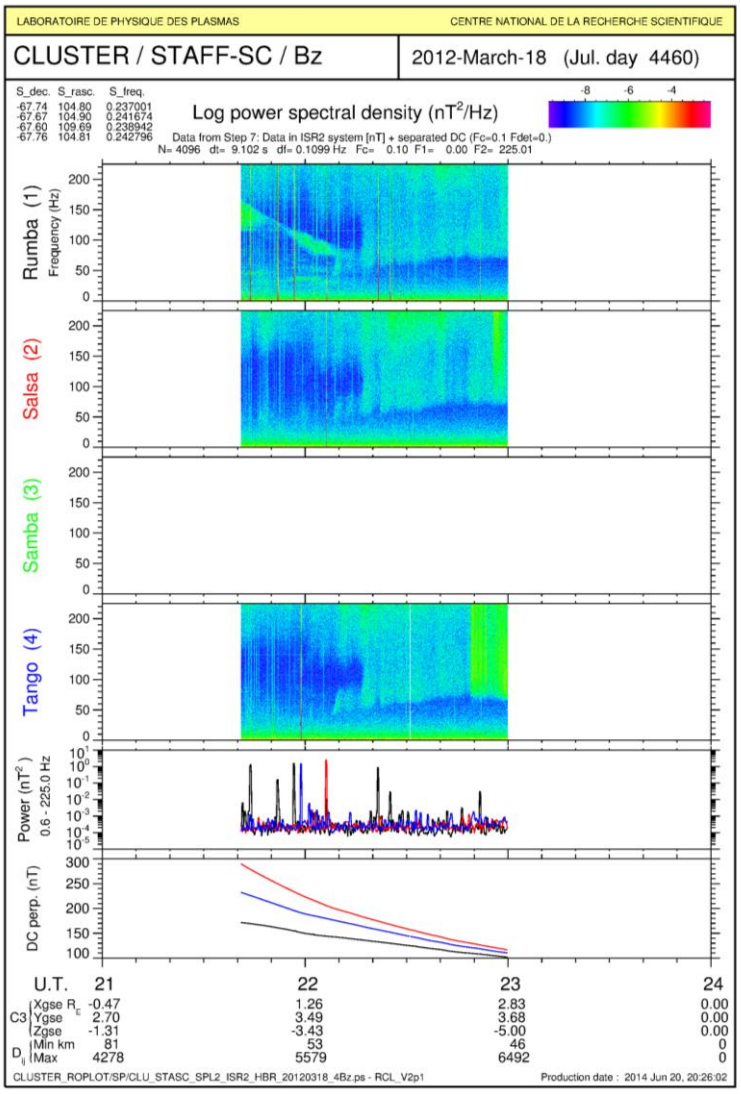

Figure 5: Example of CS data obtained with hatched telemetry in HBR mode

As expected, there is some data only in NBR mode and not in HBR mode.

7. Results of Cross-Calibration Activities

Plots hereafter have been presented at various Cross Calibration meetings. All main results have been summarised hereafter.

7.1 Comparison of STAFF-SC Spin plane DC field with FGM

7.1.1 Case studies

The STAFF/FGM comparison plots below have be presented at the *1st Cross-Calibration Workshop, 2006, ESTEC*, and at the 8th *Cross-Calibration Workshop, Kinsale, Ireland, 28-30 October 2008*.

A first problem was identified after launch: the perpendicular DC-field measured by the spinning spacecraft at the spin frequency was not the same from S/C #1 than from the other S/C: The difference was of ~ 8 to 20 % with respect to FGM. S/C# 1 gave always lower values than other S/C by ~10%, and the difference was confirmed by FGM.

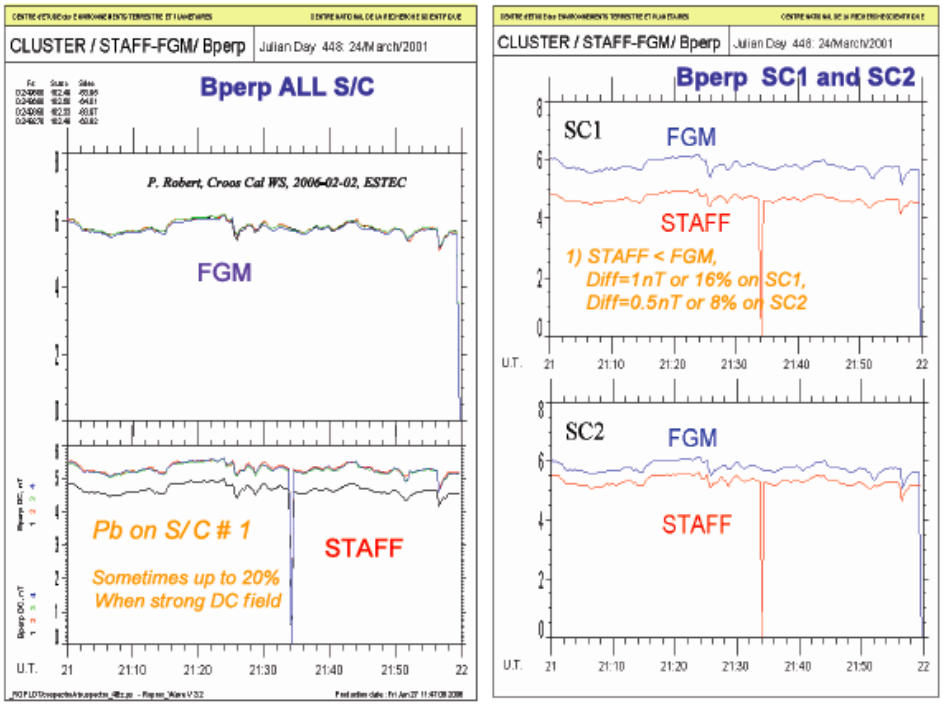

Figure 6: Comparisons of the modulus of the DC field in the plane perpendicular to the spin axis.

Left: comparison of the perpendicular components between the four spacecraft. Top panel is for FGM and bottom for STAFF-SC. Right: comparison of FGM and STAFF-SC for C1 and 2.

After correction of the transfer functions, the FGM/STAFF comparison gives the following results, shown in

Figure 7. Now the agreement is good on this case study for the modulus of the DC field perpendicular to the spin axis.

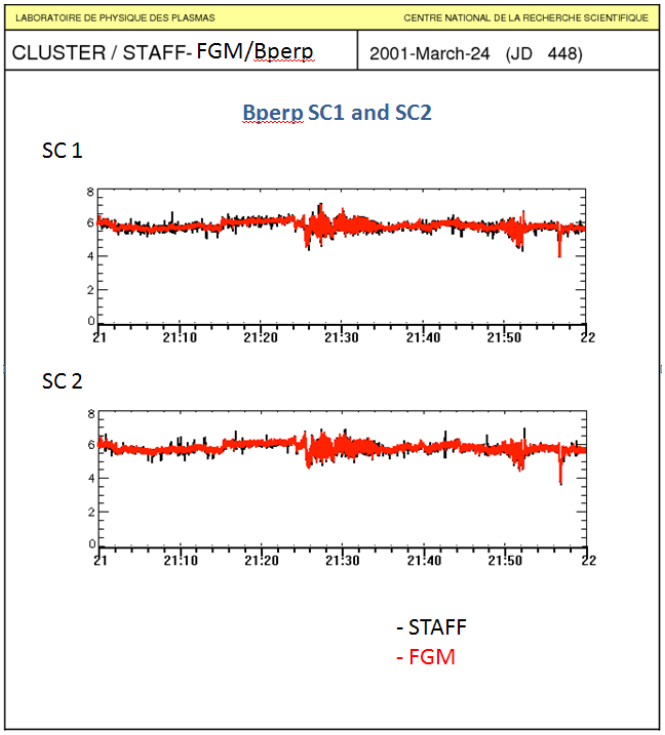

Figure 7: Same as right panel of Figure 6, with the corrected transfer function

This plot has been done with high resolution data. One can see the good agreement between STAFF and FGM data.

Results of a detailed study showing the components of the DC field in the spin plane for both STAFF and FGM, before and after the transfer function correction are given in Figure 8: STAFF (black) and FGM (red) comparisons with the old (left) and the corrected transfer function (right), for Bx, By, Bperp and Phi components., for S/C 1 and S/C2.

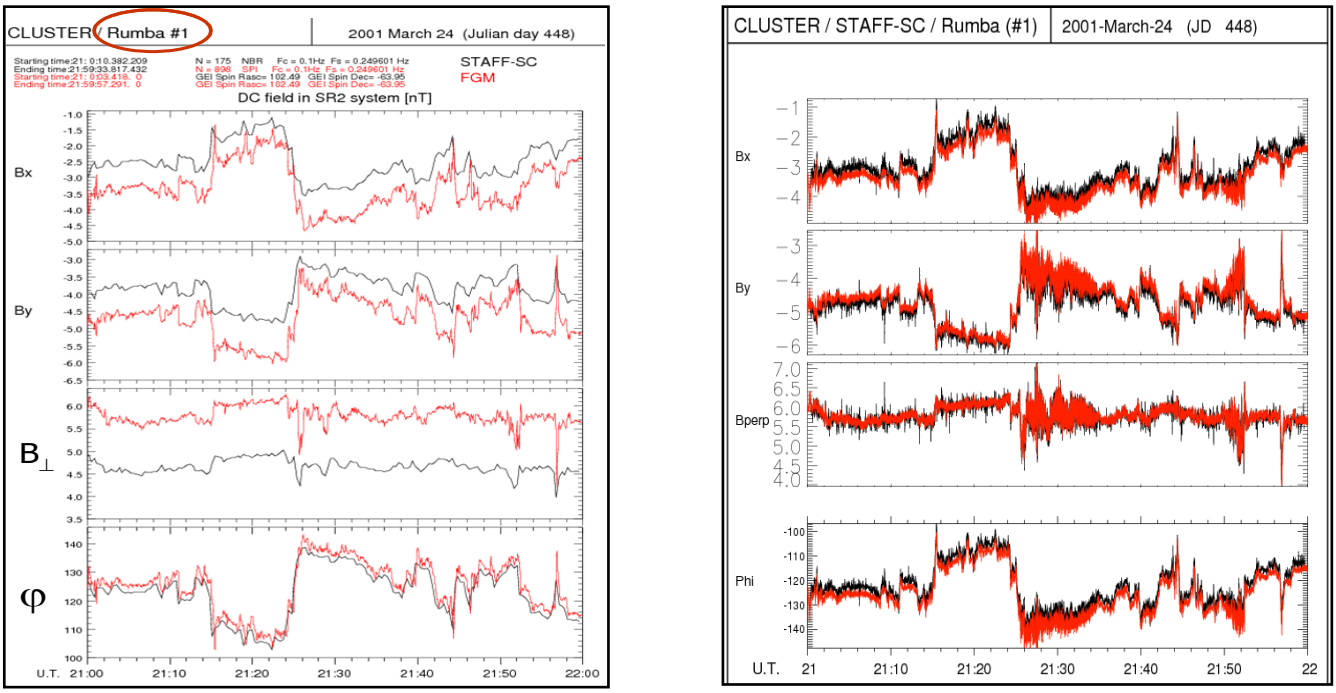

Figure 8: STAFF (black) and FGM (red) comparisons with the old (left) and the corrected transfer function (right), for Bx, By, Bperp and Phi components.

The good agreement for the corrected transfer function is clear.This new plot has been done with the high resolution FGM data and the continuous CWF STAFF-SC data.

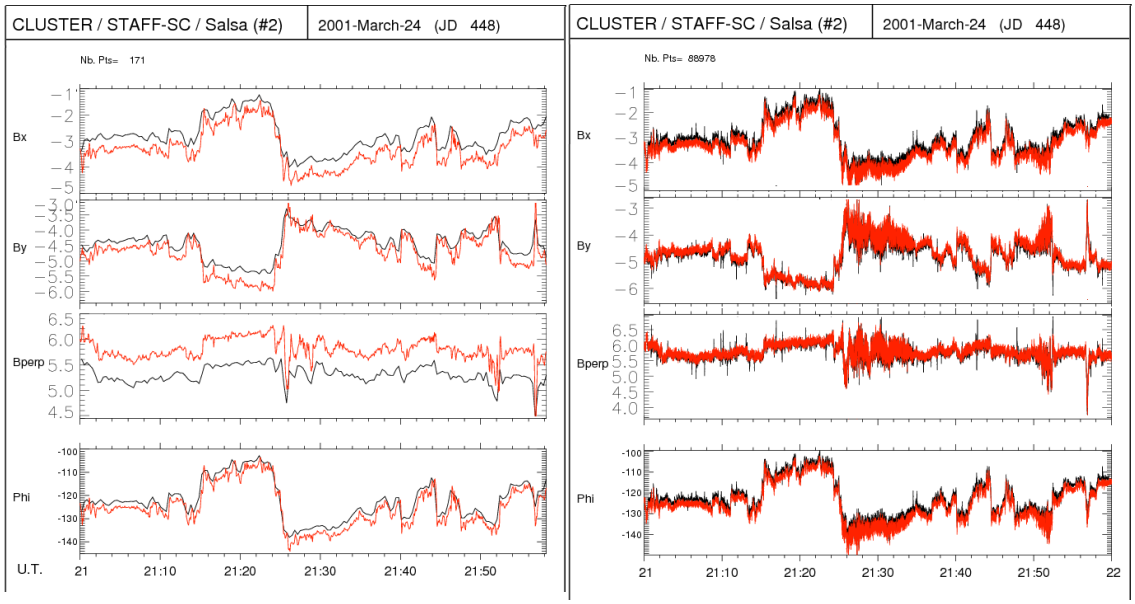

Figure 9: same as Figure 8, for S/C 2

7.1.2 Statistical study for all S/C

To confirm the above results, a statistical study has been done on more than 30 cases, covering 6 years of Cluster mission, in various conditions. Results are shown below (S/C#1,2,3,4 in Black, R,G,B).

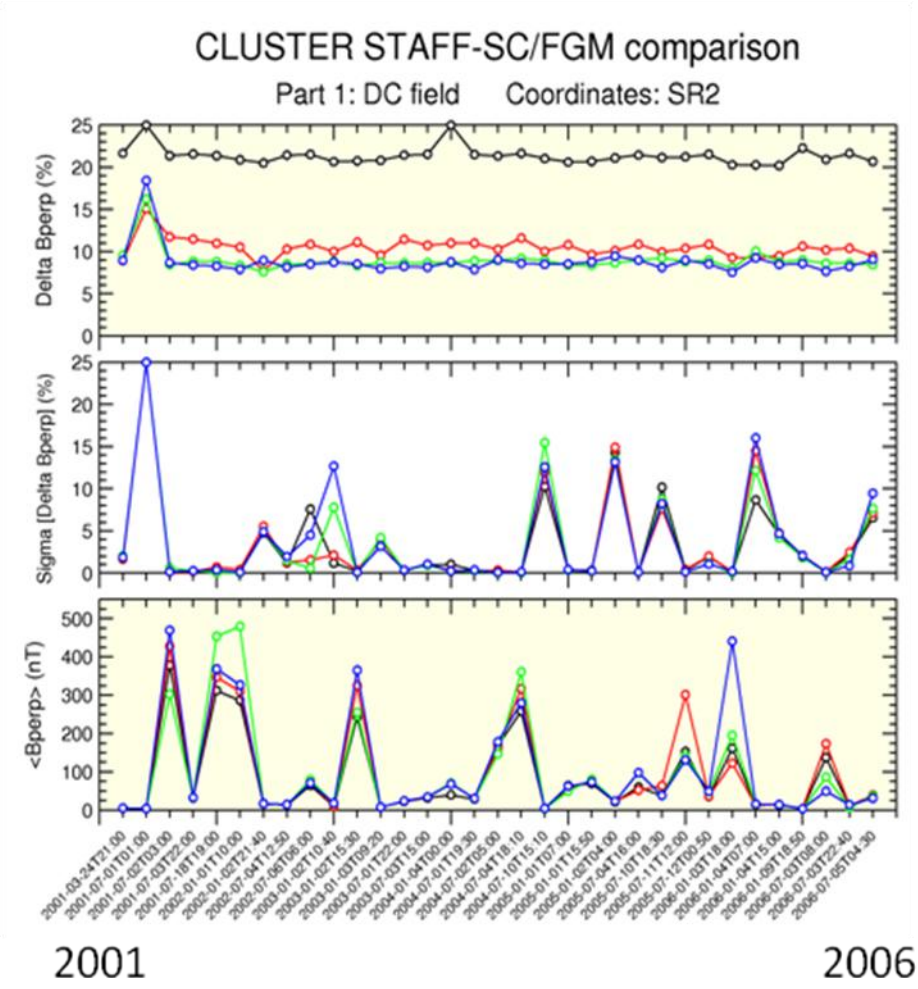

Figure 10: Evolution with time of STAFF and FGM comparison for DC field data in the spin plane obtained with the old transfer function

⇒ These results show that the difference on the DC fields was always ~21% for S/C#1 (with STAFF lower than FGM), and ~10% for S/C#2,3 and 4.

First panel shows the relative difference $\Delta B_\perp / B_\perp$ in %, where we can see that this difference is roughly constant for each spacecraft during the 10 years studied.

Second panel shows the standard deviation of $\Delta B_\perp / B_\perp$ which is between 0.5 and 5%, except one point at 12%, but which correspond to a very low $B_\perp$, so $\Delta B_\perp / B_\perp$ become relatively high taking into account the accuracy of the measurement.

Third shows the amplitude of the $B_\perp$ DC field for each event, from a few nT to 500 nT.

This series of results have led us to go back to the old calibration files and to the ground calibration facility.

This has led to two different results. First spacecraft 1 had been calibrated with a different current loop than the other spacecraft. Measurements of the 2 different loops characteristics explained the difference of about 10 % at 0.25 Hz, the difference decreasing progressively with increasing frequency, being null at 8 Hz. It has been decided to apply to the C1 data the mean transfer functions of C2, C3 and C4.

Second, looking at the equipment, it was found that the calibration loops are no longer a perfect circle; new tests have been done with new and accurate sensors. A further correction of about 7 dB to apply to the previous measurements has been identified. The results of the use of the new transfer functions are shown in what follows.

When applying the corrected transfer functions to the same data set, one finds the results given in Figure 11: Same as Figure 10 with the corrected transfer functions. The difference between FGM and STAFF are now of the order 1%:

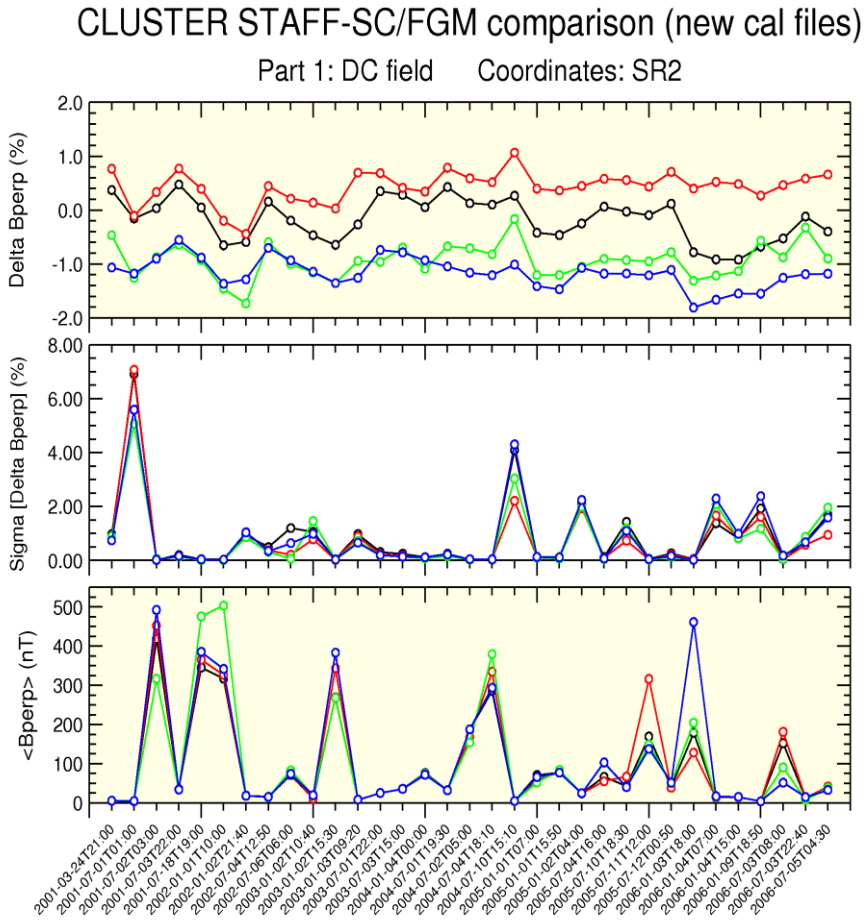

Figure 11: Same as Figure 10 with the corrected transfer functions. The difference between FGM and STAFF are now of the order 1%

⇒ **In conclusion**, these new results show that the new transfer functions give results almost identical to FGM ones (within 1 %), for strong and weak signals and for six years of Cluster data.

⇒ Independently of the transfer function issue, one should notice the stability of the instrument performances with time.

In order to validate this last study, statistics were performed over 10 years of STAFF-FGM DC field comparison. Altogether, 58 events have been chosen, in four various conditions each year:

- Low DC field, low ULF activity,
- Low DC field, high ULF activity,
- High DC field, low ULF activity,

- High DC field, high ULF activity.

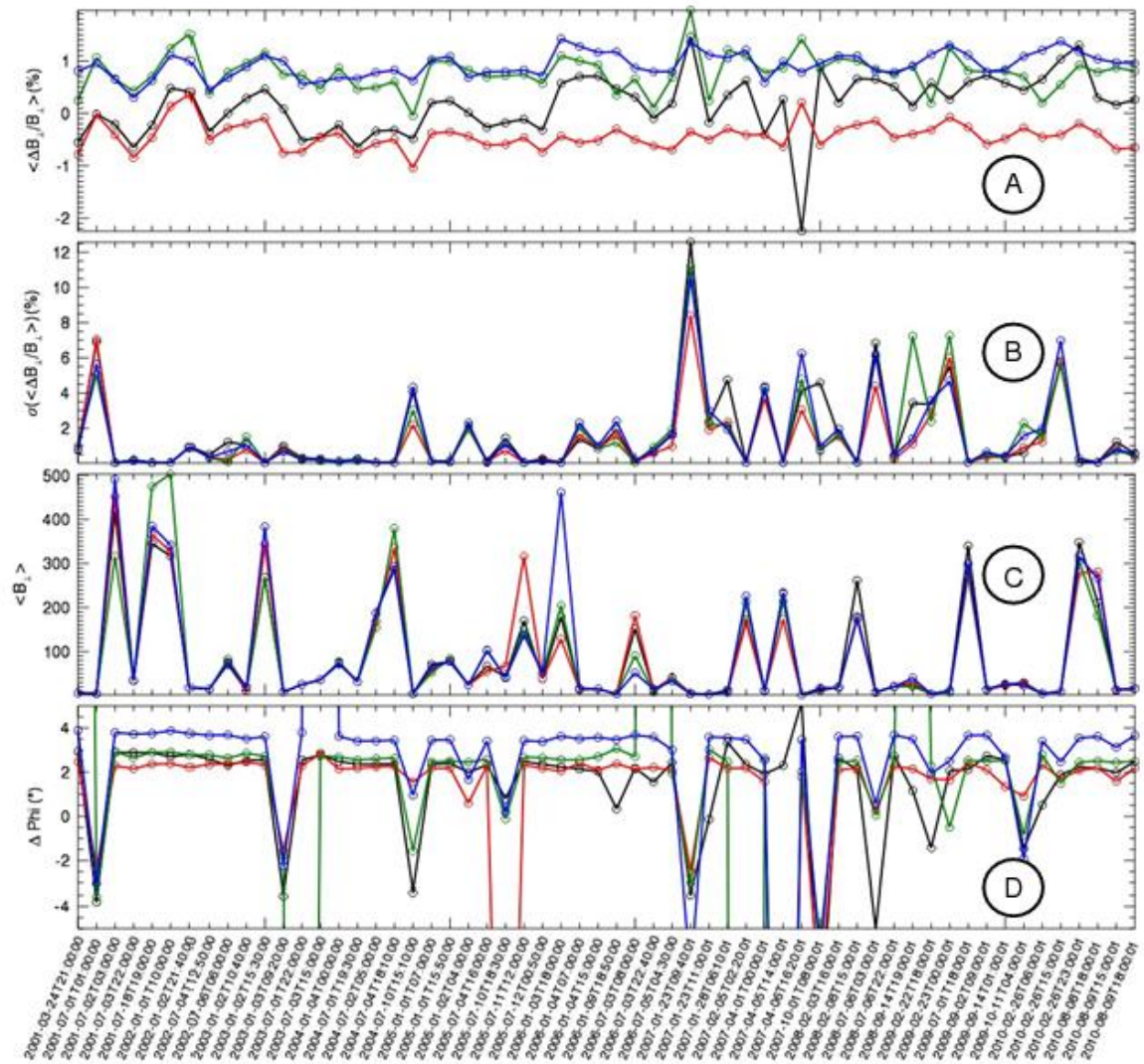

Figure 12: Statistic over 10 years of STAFF-FGM spin plane DC field comparison for the four spacecraft (black, red, green, and blue for spacecraft 1, 2 3 and 4 respectively)

Panel A shows the relative difference $\Delta B_\perp / B_\perp$ in %, where we can see that this difference is roughly constant for each spacecraft during the 10 years studied.

Panel B shows the standard deviation of $\Delta B_\perp / B_\perp$ which is between 0.5 and 5%, except one point at 12%, but which correspond to a very low $B_\perp$, so $\Delta B_\perp / B_\perp$ become relatively high taking into account the accuracy of the measurement.

Panel C shows the amplitude of the $B_\perp$ DC field for each event, from a few nT to 500 nT.

And last, panel D gives the phase difference of the $B_\perp$ component in SR2 system.

Concerning the relative stability of $\Delta B_\perp/B_\perp$, we can see that it is independent of the magnitude of the DC field, whatever the level of ULF activity. Furthermore, for each spacecraft, this difference remains constant all over the studied 10 years. This is an important result, because

it shows that the transfer function remains constant from the beginning of the mission until present. This result could be confirmed by a dedicated study of the onboard calibration signals.
Another important result is the difference from one spacecraft to another: In fact, the best result seems be obtained for the S/C #1, where the transfer function has been obtained by the averaging of the 3 others (S/C2, S/C3 and S/C4). This result is thus directly directed by the estimate of the transfer function on the ground, and gives an estimate of their accuracy (see section 3). The choice has been done to keep each of the 3x4 transfer function slightly different, but, as these tables should be all theoretically identical, another choice could have been to set all tables to the S/C#1 average table.

Concerning the direction, most of the time this $\Delta\varphi$ difference is between 2 and 4°.
Nevertheless, for some cases, the sign of this difference changes and is between -2 to -4°. This change is not explained up to now.

7.2 Comparison of STAFF-SC waveform with FGM

7.2.1 Classical method and old transfer function

Plots below directly compare the STAFF-SC calibrated waveform (NBR) with FGM data, in the SR2 system (*1st Cross-Calibration Workshop, 2006-02-02, ESTEC)*.
STAFF spin plane components are differently affected by the spacecraft spin. SR2 frame has been also chosen as it does not mix the XY spin plane components, and the parallel Z component. To remove the remaining spin effect, waveforms (STAFF and FGM) are filtered between 1 and 6 Hz.

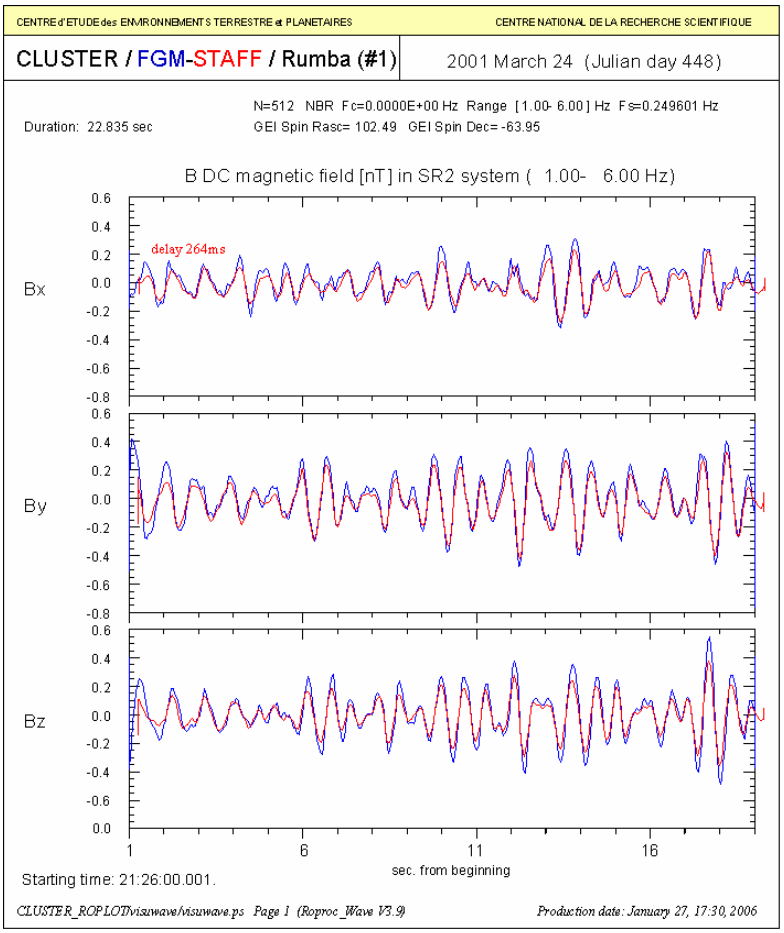

Figure 13: STAFF/FGM comparisons at waveform level

Results are rather satisfactory, particularly concerning the shape of the waveform, which correspond to a wave at ~ 2 Hz.

For another example, there is a zoom on the phase comparison, which has not changed with the updated transfer function, see Figure 8.

⇒ In this event using the old transfer function, we found the same difference of ~ 20 % on the amplitude for S/C#1. Conclusions remain the same for other S/C.

It is also possible with STAFF to obtain the no filtered waveforms in the spin plane, including DC part. This is the example above, where we apply an arbitrary offset to a better visibility:

Bx = - 4.5 By = - 5. Bz = +0.5

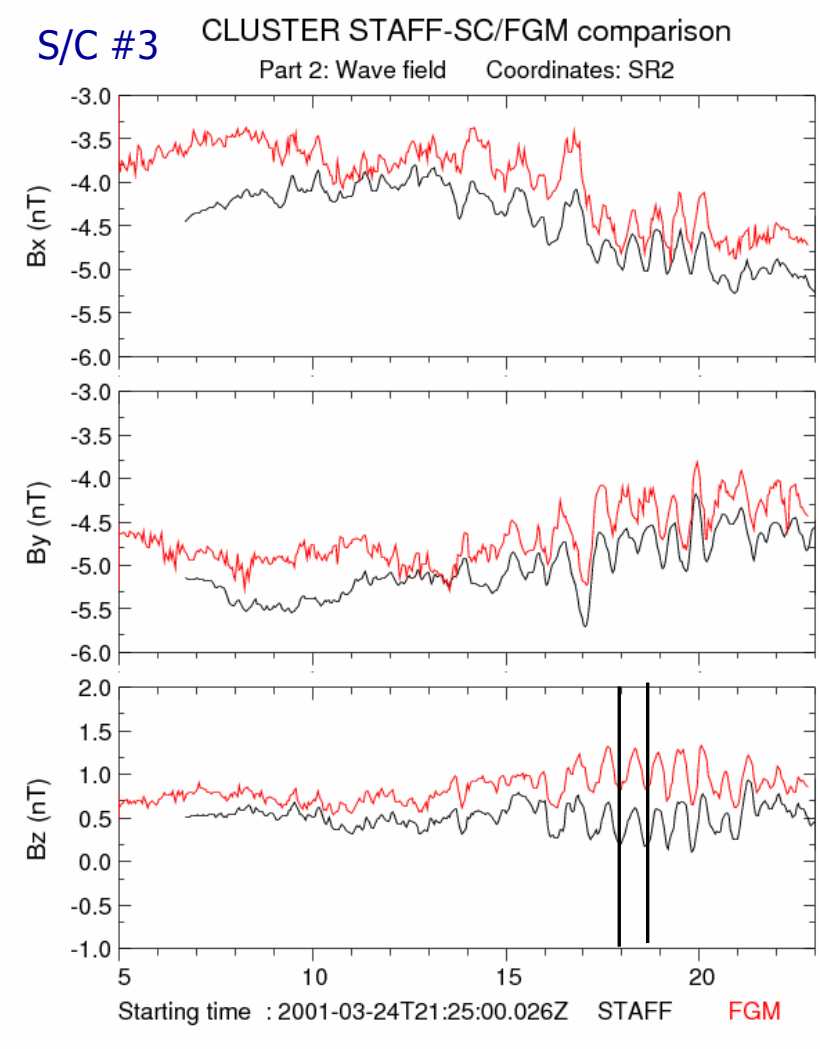

Figure 14: Same as Figure 13 for another event.

Results show a very similar shape, and STAFF fluctuations amplitude at ~1 Hz are always ~10-12% lower than the one of FGM.

⇒ Once again, we got the same conclusion at 1 Hz than for the DC field.

7.2.2 Continuous calibration method and new transfer function

Results given below have been shown in the *15th CAA Cross-Calibration meeting, London, April 2012.*

The Calibrated Wave Forms (CWF) using the new (corrected) transfer function are delivered to CAA in both GSE and ISR2 frames. An example of the CWF product is given below. In this example the data are in GSE frame, filtered above 0.5 Hz to avoid all spin effect and have a range where sensitivity is good. Note that in SR2 system the 2 DC components in spin plane are also delivered.

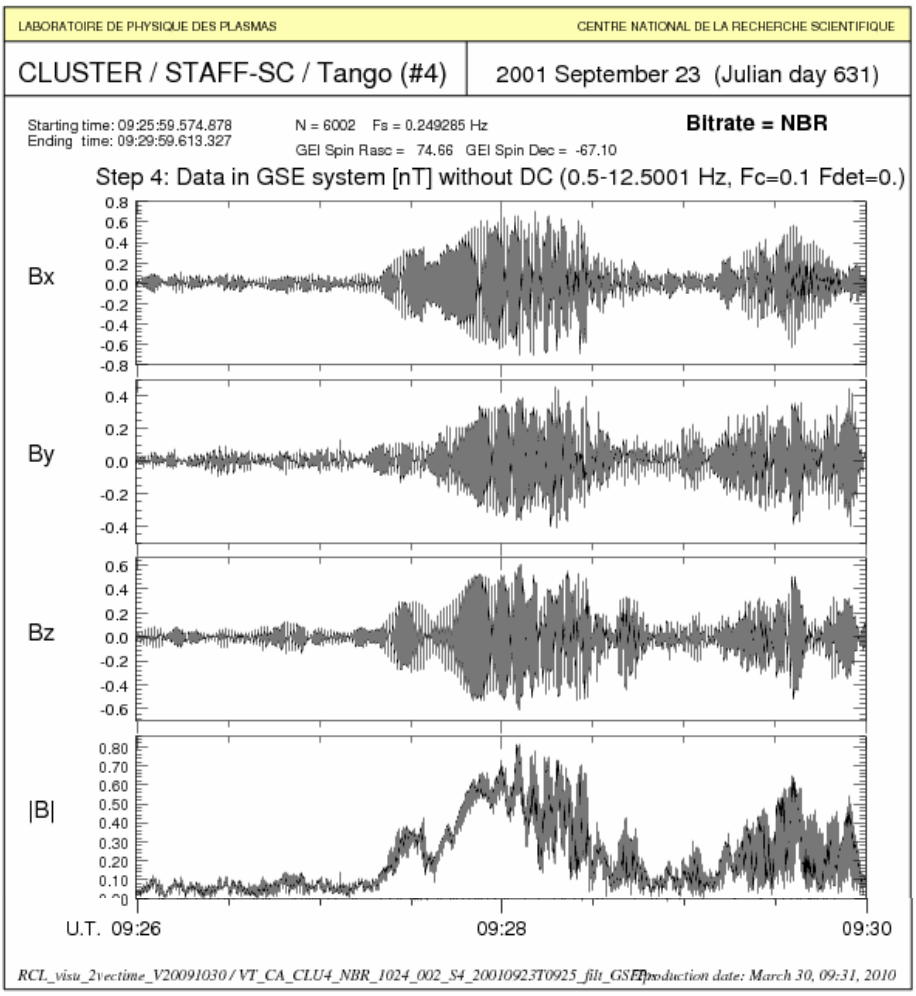

Figure 15: example of the continuous calibration method results.

The figure below presents a further example of comparison between the calibrated waveform delivered to CAA and FGM data. FGM and STAFF data now agree within 1%.

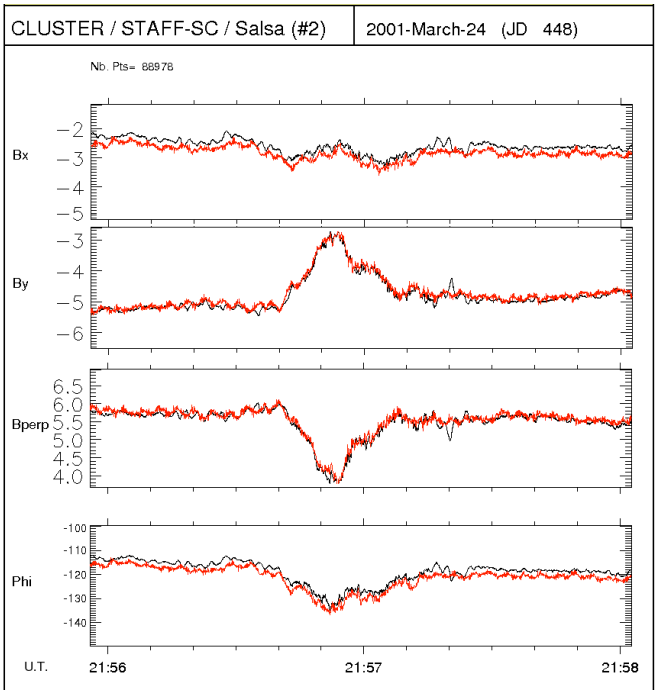

Figure 16: comparison STAFF/FGM for a short time scale event.

7.2.3 Comparison at 1Hz

Figure 17 shows an event with an almost monochromatic wave at low frequency (~1 Hz) superimposed to a low DC variation. On the left, one can see a constant difference of ~1% on the $B_{\perp}$ component, as expected, and a phase difference of ~4°. The zoom (on the right) shows still the same agreement on the DC part, both in amplitude and phase. To see a more precise comparison for the component at 1 Hz, we shift the FGM data of 3.3 nT (1.1 %) to have a better superimposition of the two curves (Fig. 18). The result is rather satisfying, a good fit being found at a first glance, but a spectral analysis is required to get a better estimate of the difference.

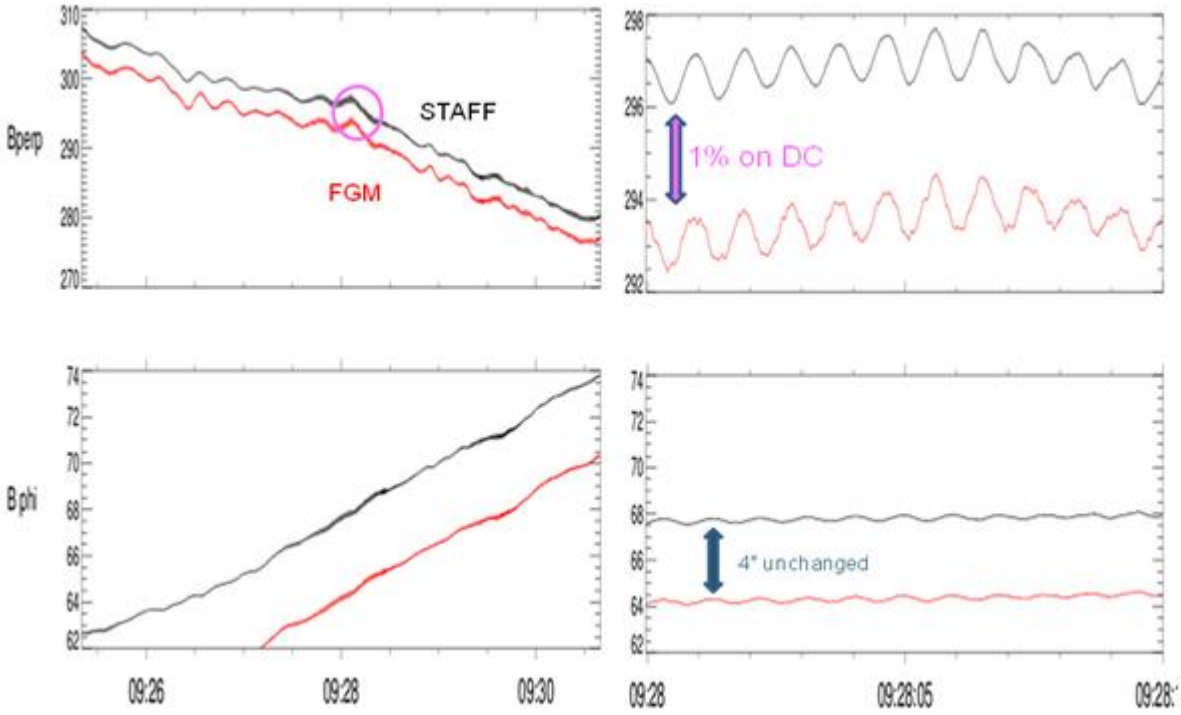

Figure 17: comparison at 1 Hz (CLUSTER/Tango (#4) 23 September 2001).

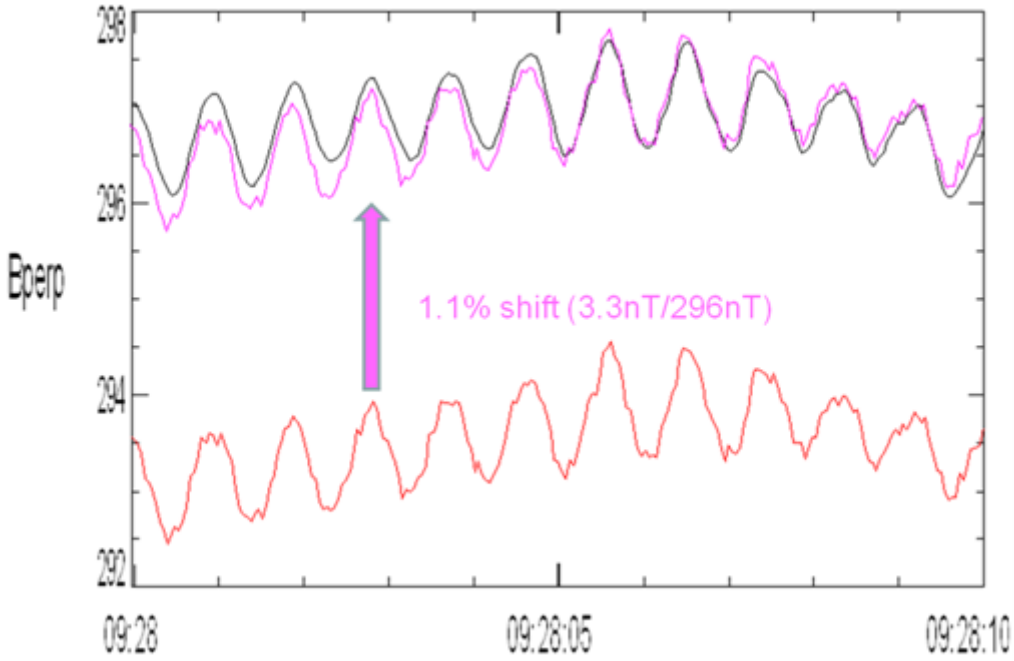

Figure 18: Wave at 1 Hz, STAFF-FGM superimposed.

7.2.4 Comparison at 6 Hz

The following example corresponds to another almost monochromatic wave at ~6 Hz, always superimposed to a low DC variation (Fig. 13). The wave occurs at ~ 09:39 UT on By. Agreement on DC files remains the same ($\Delta B/B < 1$ %, $\Delta\phi \sim 3°$).
By zooming on the wave (Figure 19) we can identify a ~ 6Hz wave whose both amplitude and phase seems to be in good agreement, but as previously, a spectral analysis is required to get more details.).

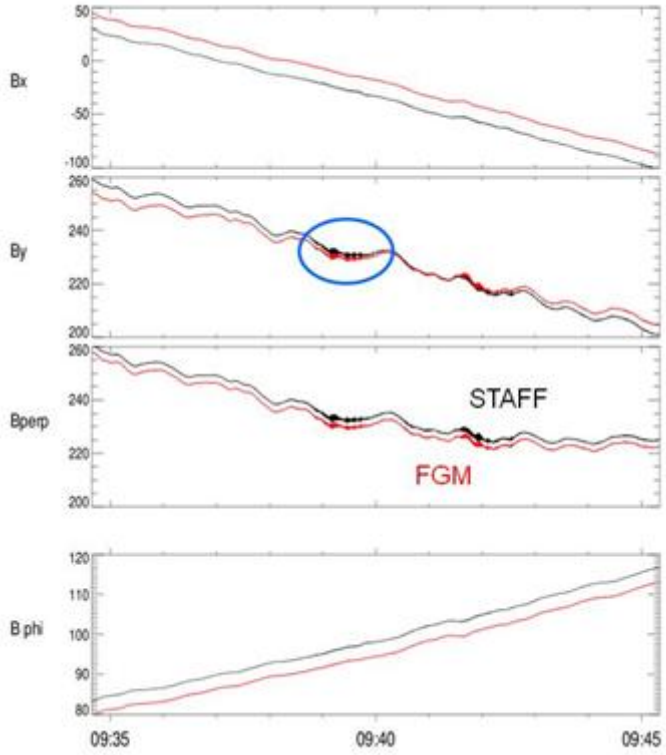

Figure 19: Wave comparison at 6 Hz (CLUSTER/Tango (#4) 23 September 2001. 14th CAA

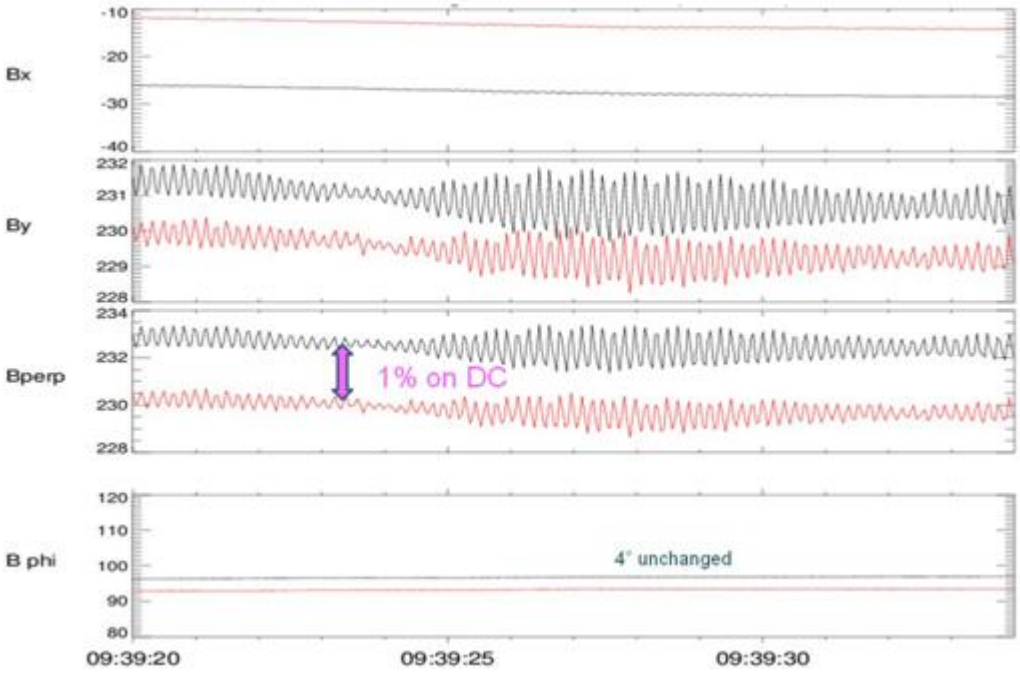

Figure 20: Zoom on wave comparison.

7.3 Comparison of STAFF–SC spectra with FGM

7.3.1 STAFF-SC/FGM sensitivity

Figure 21 shows a spectrum of STAFF and FGM done during a very quiet period, which means that these two curves can be considered as the sensitivity of the two instruments. The two curves cross at ~ 0.7 Hz, that is to say that at this frequency the two instruments have the same sensitivity. Below 0.7 Hz, FGM is not only more sensitive, but gives of course the three components of the DC field contrary to STAFF. Above 0.7Hz, the search-coils are more sensitive and can detect event of smaller magnitude. This leads to choose one experiment rather than the other, according to whether you look at DC or at waves, and for waves to which frequency range you want to focus on. In fact the two experiments are quite complementary.

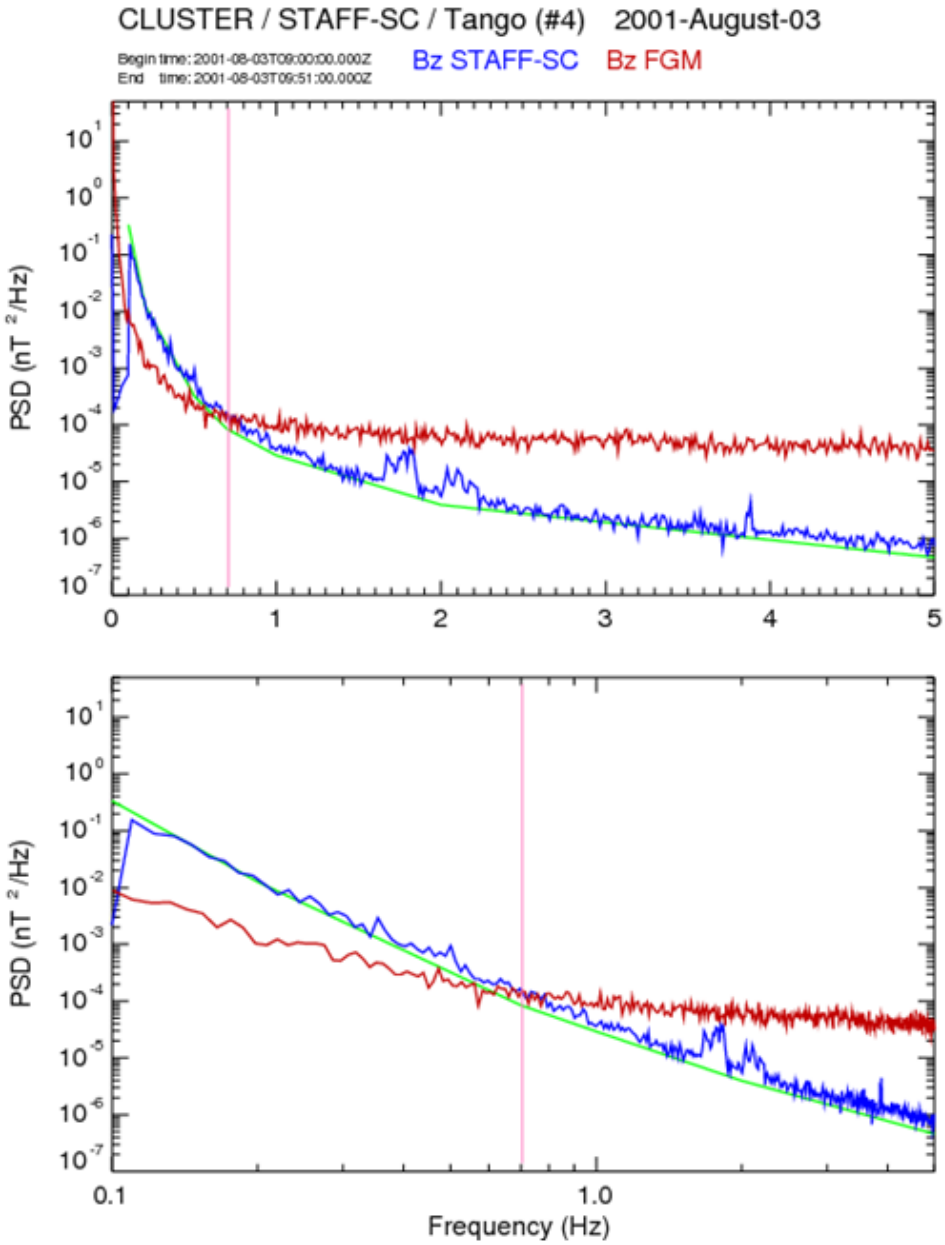

Figure 21: STAFF-FGM spectra comparison for a very low power event, to show respective sensitivity

7.3.2 1 Hz event

Figure 22 shows the FGM and STAFF spectra corresponding to the waveform event of Fig. 11. The strong peak at 1 Hz spreads from 0.5 to 1.5 Hz, and the accordance between the two instruments is very good, even for the second peak at ~ 2.5 Hz. To quantify the exact difference, a dedicated study should be done, requiring filtering of the high frequencies, spikes removing and Shannon interpolation for the STAFF-FGM resampling. The noise above 3 Hz is higher for FGM, as expected; nevertheless it is above the sensitivity shown on Figure 22: STAFF-FGM Spectra comparison for event at 1 Hz..

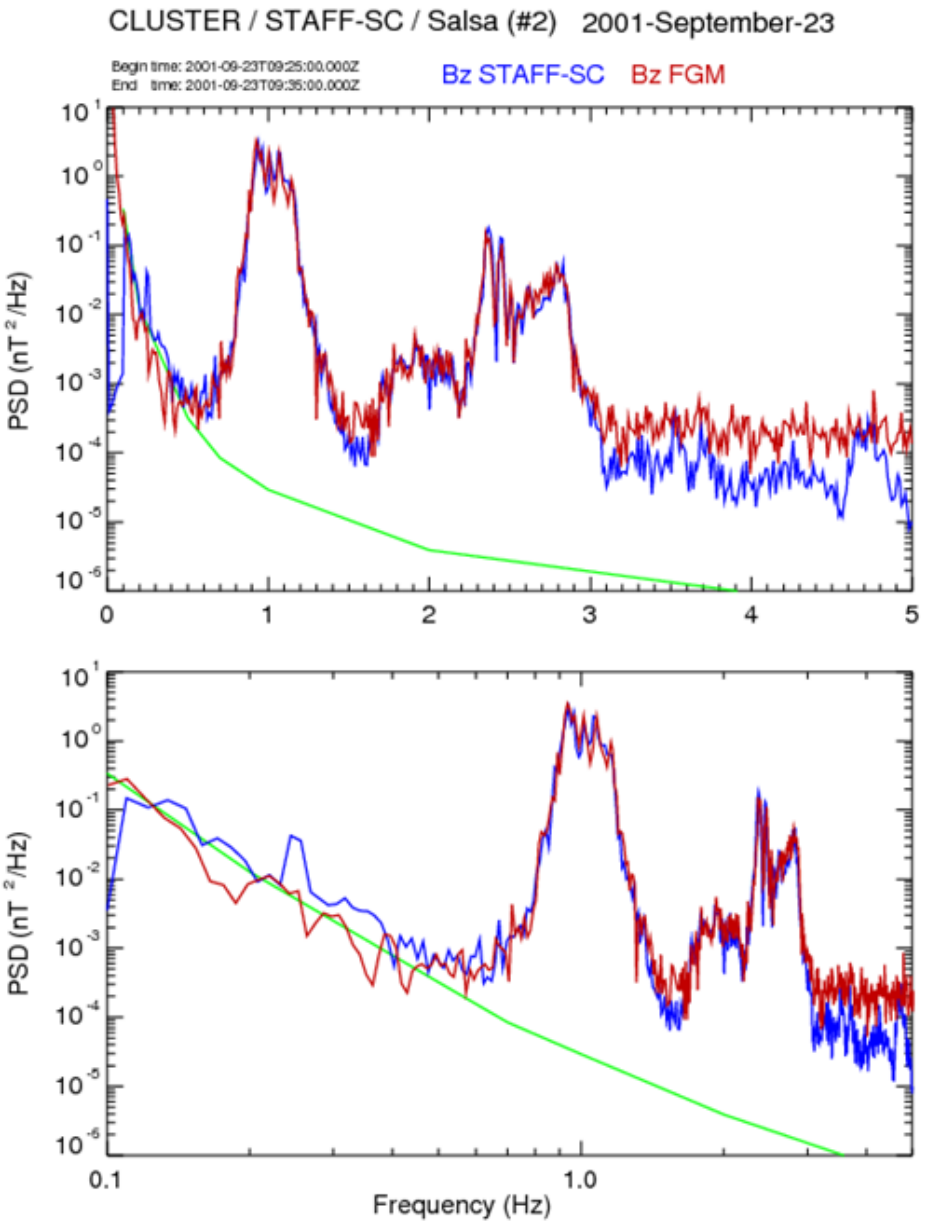

Figure 22: STAFF-FGM Spectra comparison for event at 1 Hz.

7.3.3 6 Hz event

Figure 23 shows the spectra corresponding to the waveform event at 6Hz of Figure 19 and Figure 20. As above, the strong peak at 6 Hz spreads from ~ 4.5 to 6.5 Hz, and shows a very good agreement between STAFF and FGM. Nevertheless, the second peak at ~ 7.75 Hz is not recorded by FGM, its sensitivity being not sufficient at this frequency. On the other hand, low frequency below 0.4 Hz is not recorded by STAFF. This example is also a good illustration of the respective interest of the two instruments.

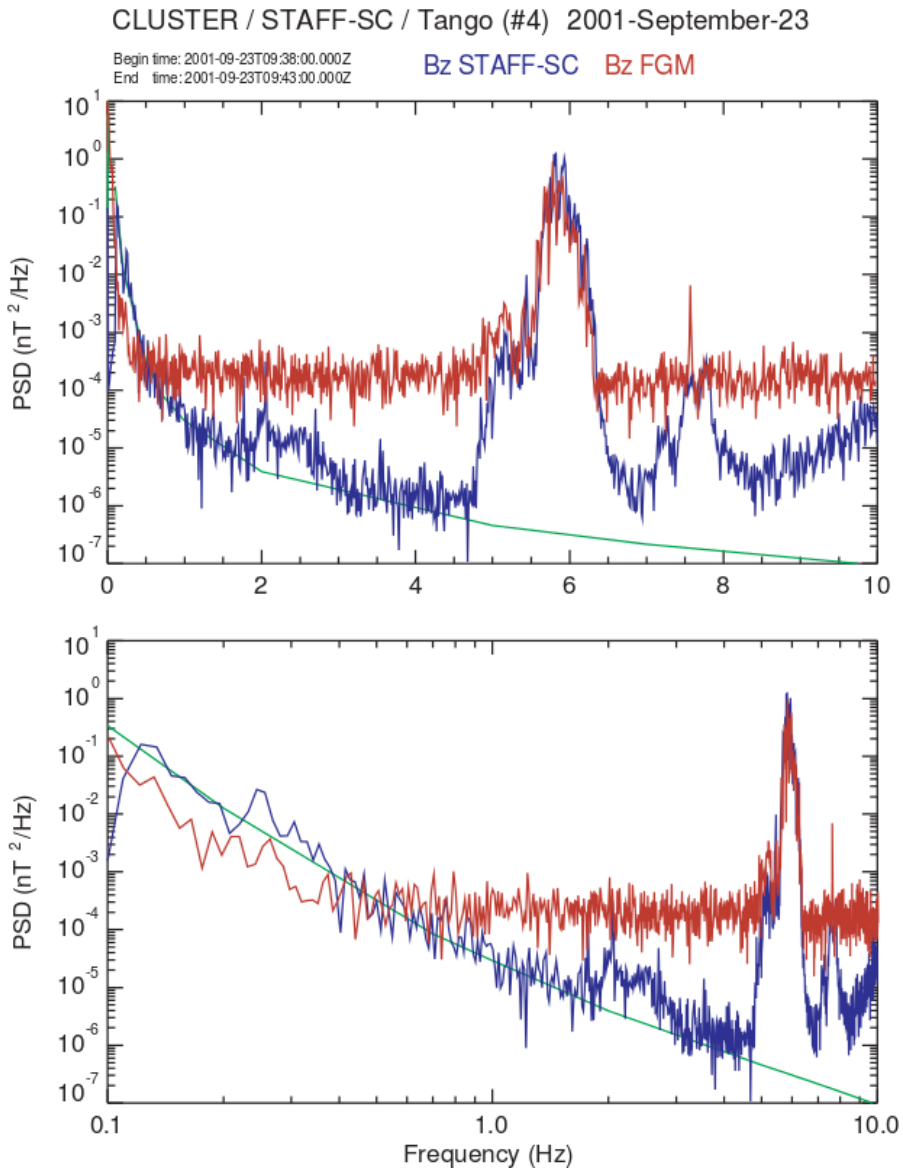

Figure 23: STAFF-FGM Spectra comparison for event at 6 Hz.

7.3.4 Wide frequency band event

Figure 24 shows a strong signal over the whole frequency bandwidth. The accordance is very good between 0.1 and ~ 4 Hz. Above 4 Hz, the power spectral density (nT2/Hz) of STAFF and FGM differs by nearly a factor of 2. Since the event is strong, the two instruments are widely

above their sensitivity (the green line corresponds to the STAFF-SC sensitivity). Furthermore, this is STAFF which is above FGM. A deeper study must be done to explain this.

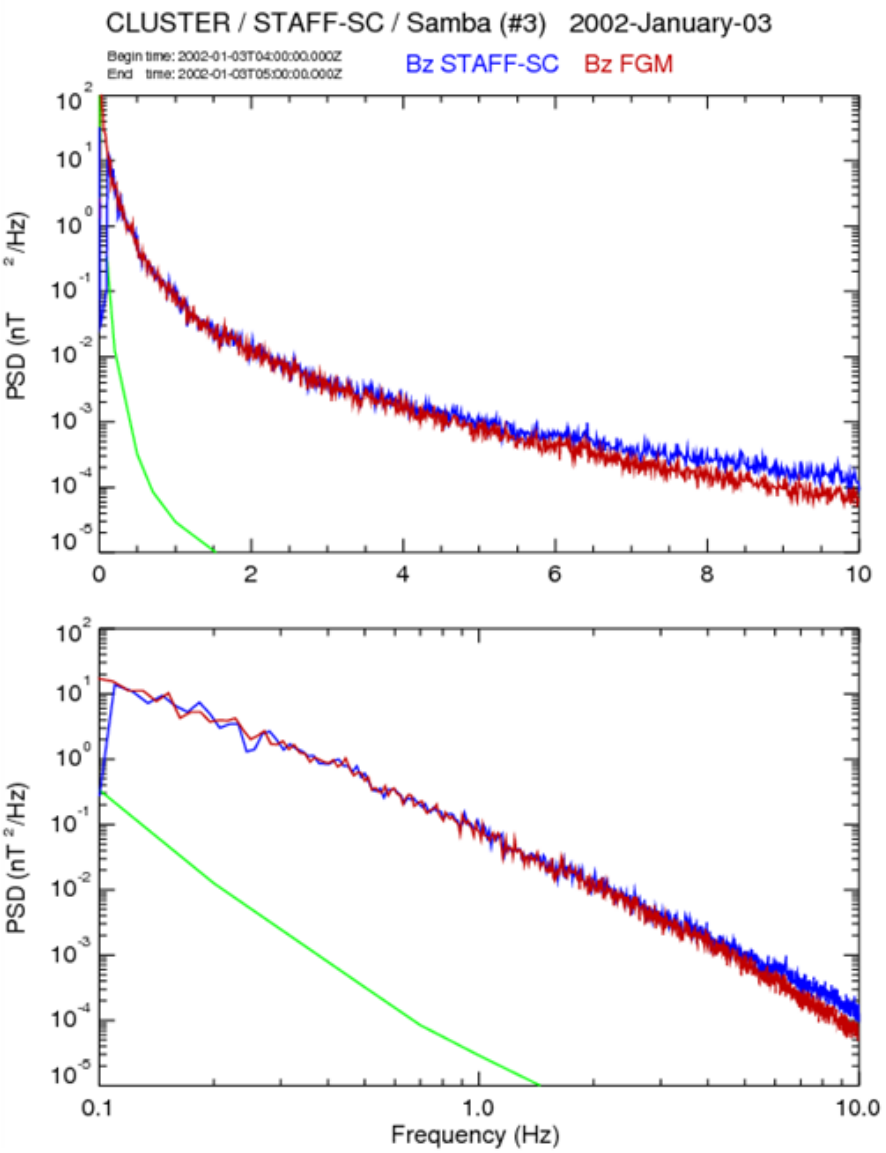

Figure 24: STAFF-FGM Spectra comparison for a large frequency band event.

7.4 Spectrum continuity between STAFF and FGM

Hereafter plots come from [9], and show a rather good agreement between the slope of the STAFF-SC spectra (NBR) and FGM, within a common frequency range of about 0.6 to 3 Hz. Plots show also an abrupt change of the slope around 1 Hz, but the spectra continuity between STAFF and FGM is clearly visible. Although the logarithmic scale does not allow the estimation of the differences with accuracy as previously, said the result is still significant.

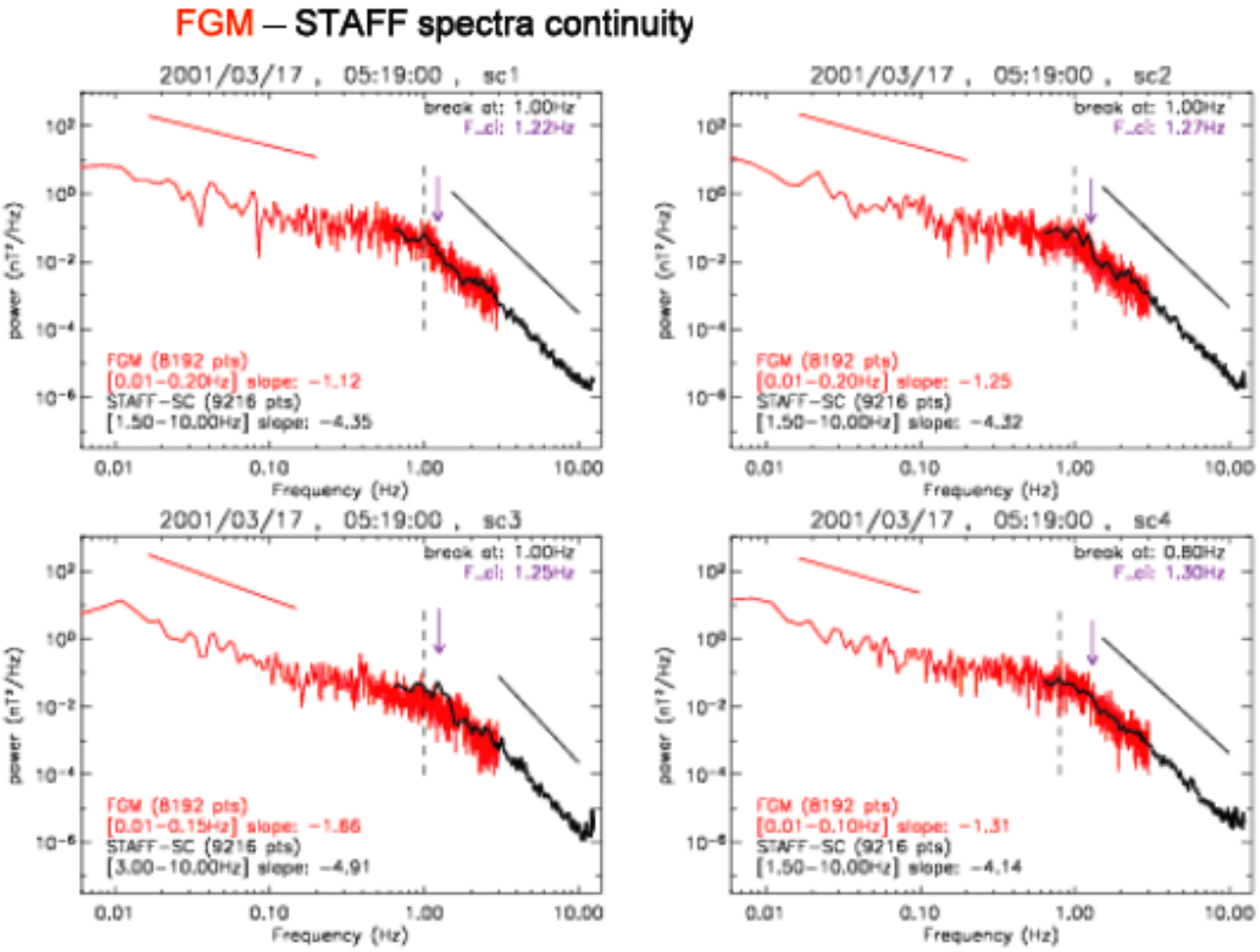

Figure 25: Comparisons of spectra coming from FGM (red) and STAFF-SC (black)

7.5 Conclusions on STAFF-FGM comparison

7.5.1 Main conclusions

All the previous differences observed between STAFF-SC and FGM have mostly disappeared with the correction of the search coil transfer functions. There is no longer a difference between S/C 1 and the other spacecraft. The residual difference between STAFF-SC and FGM is now of the order of 1 – 2 % in amplitude and about 2-3 ° in phase. It is not expected to reach a better agreement in the future.

7.5.2 Limitation of STAFF-FGM comparison at low frequency

The DC part of the magnetic field can be estimated by STAFF-SC thanks to the Doppler effect, as seen previously. But since the transfer function is null at zero frequency, there is a gap in the observed spectrum, depending on the wave polarization.

So, a right-handed polarized wave at spin frequency cannot be recorded by the STAFF sensor. It is seen at F=0 by the spinning sensor coordinate system because we have $F_{SR2}= F -F_{spin}$

But a left-handed polarized wave at any frequency, including DC, is recorded by the STAFF sensor because its frequency is $F_{SR2}= F +F_{spin}$

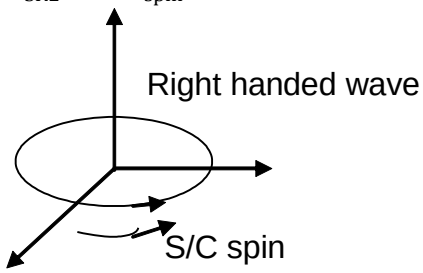

Figure 26

In conclusion, at low frequency, near the spin frequency, we cannot expect a full agreement between STAFF and FGM, except for left-handed polarized wave. This is why the CWF will be filtered below 0.6 Hz, to get data with a good accuracy.

7.6 Spectra continuity between STAFF–SC and STAFF–SA

7.6.1 General continuity

Plots below illustrate the connection between STAFF-SC spectra upper frequency band and STAFF-SA spectra lower frequency band. Level and slope are rather good, except a small discrepancy for S/C #3. Further investigations should be done.

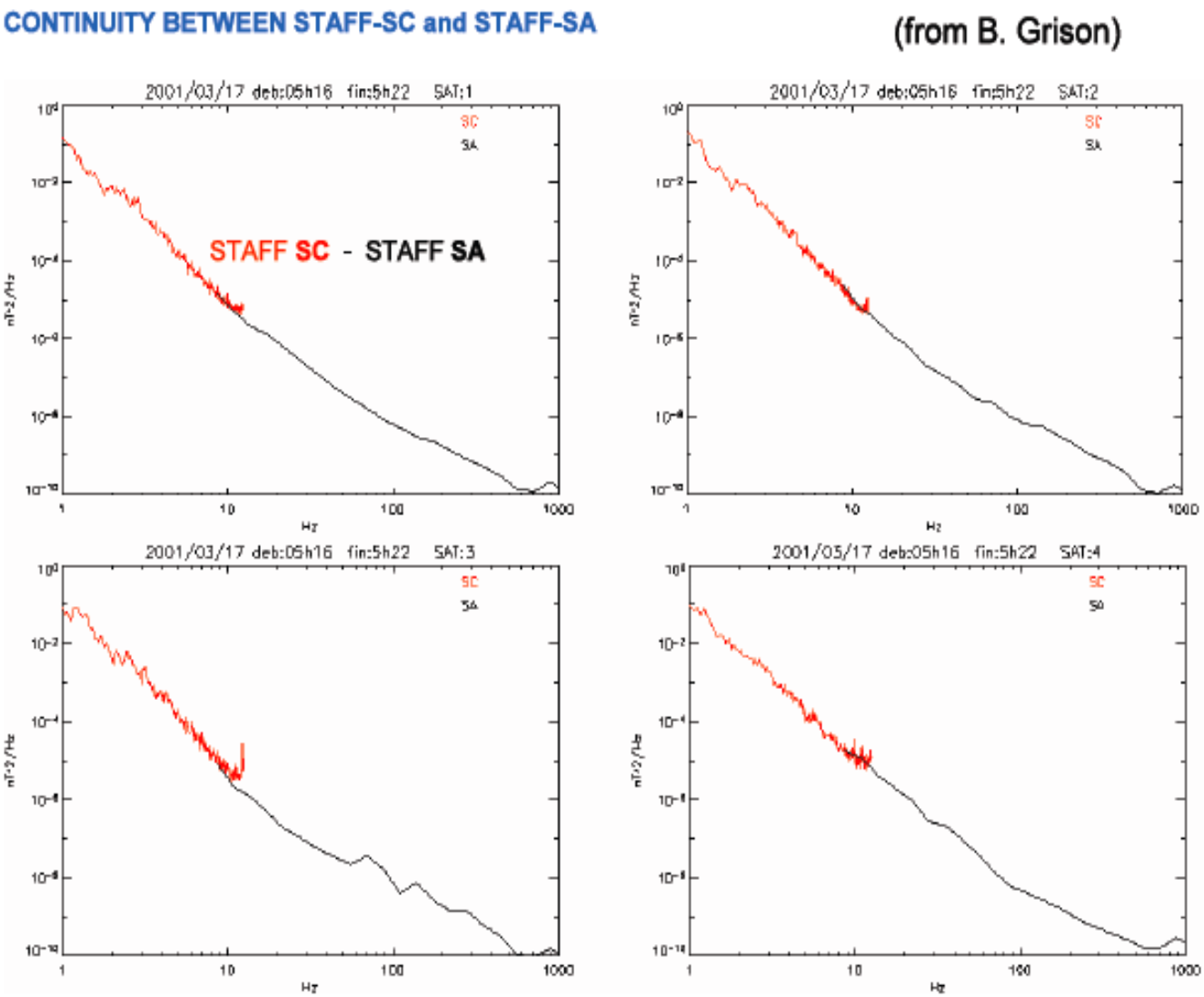

Figure 27: STAFF-SC spectrum (red) and SA (back)
Courtesy of B. Grison

7.6.2 Instrumental effect at low frequency on STAFF-SA

If the continuity between both analyses is generally good, one can on some events find, when looking in details to the data, a small apparent difference at low frequency. Figure 28, shows, for SC 1& 4, a comparison between STAFF-SC and STAFF-SA for turbulent like wave spectra: SC in the 1 -10 Hz frequency range and SA in the 8 - 300 Hz frequency range (continuous lines). The 2 sub experiments give a similar slope behaviour joined by the dotted line. But a small instrumental effect is visible, minimizing the data values of SA, between 8 and 18 Hz on S/C 1 and from 8 to 35 Hz for S/C4, S/C 2 and 3. This is under study. (See also UG § 6.3.). The 3 spectra are respectively the power perpendicularly to the main field, the power parallel to the main field and the total power.

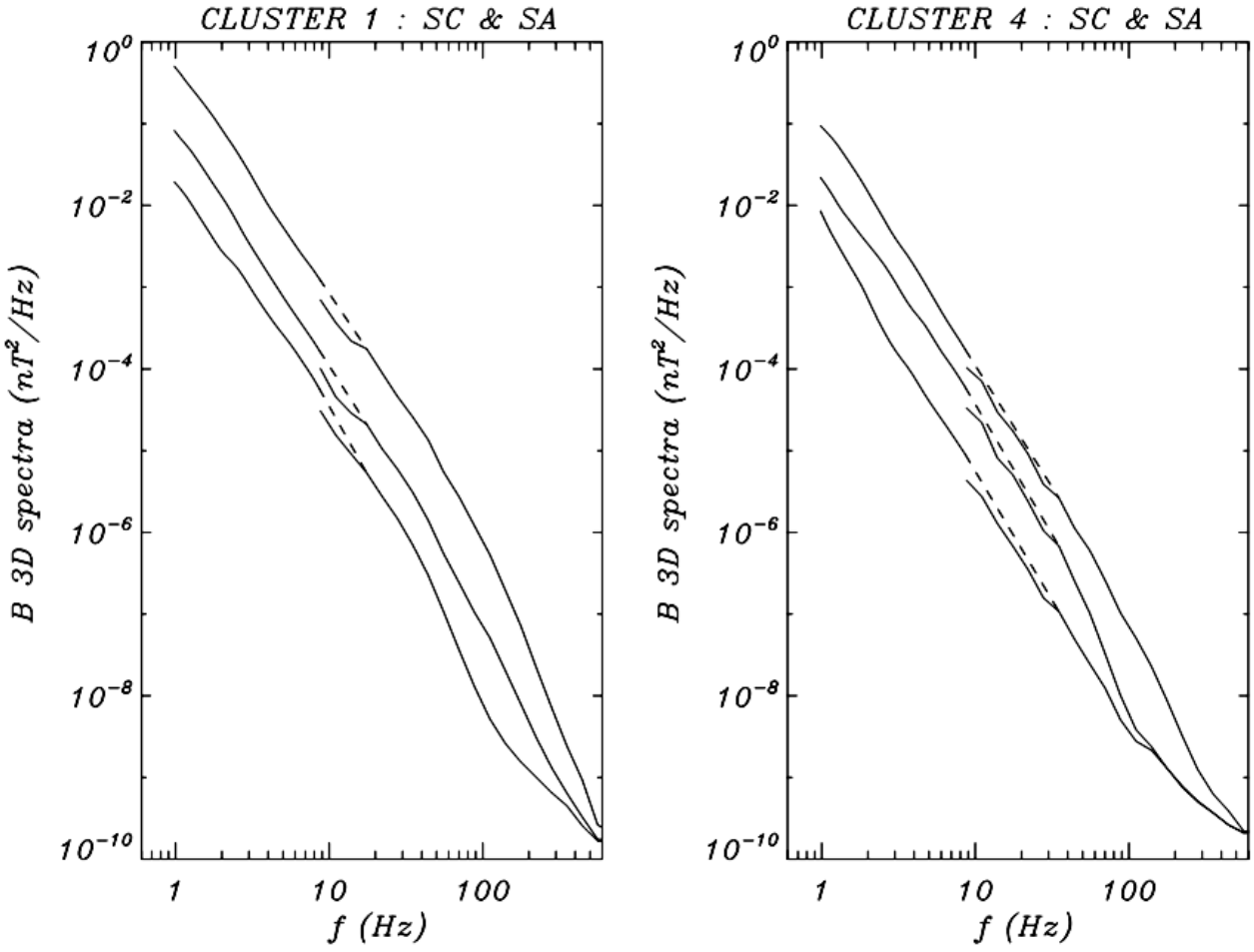

Figure 28: Evidence of small discrepancies between SC and SA at small frequencies
Courtesy of C. Lacombe and Y. De Conchy

7.6.3 Comparison using special mode of SC and SA

We can extend this comparison to higher frequencies, when SC, in HBR mode, cover the frequency range up to 180 Hz. Figure 29 (for C1) and Figure 30 (for C4) show a comparison between STAFF-SC and STAFF-SA taking benefit of a special mode commanded to get a maximum frequency overlap between the 2 analysers. The spectrum analyser has been commanded in a normal bit rate mode during a period of high telemetry rate, having then a frequency overlap between 8 and 180 Hz. The stars are for the spectrum analyser frequencies, the continuous line for the result of a wavelet analysis performed on the SC calibrated waveform. The 4 plots are for the 3 magnetic components and the total power. Both behaviours are globally similar, taking into account - as in the previous figure - the underestimation of STAFF-SA at low frequency (see above).

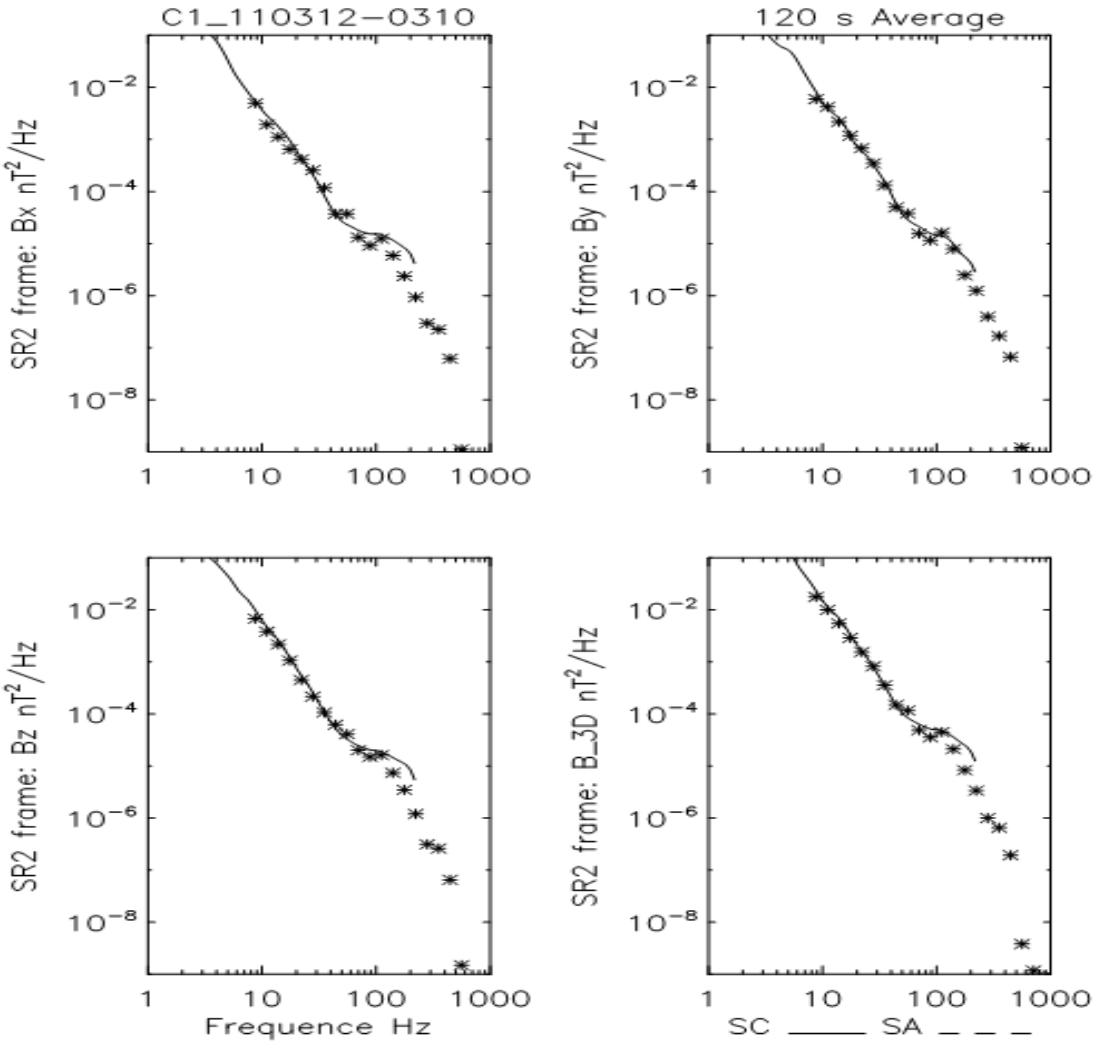

Figure 29: Combined spectra between STAFF-SC (line) and SA (cross) for SC1
Courtesy of C. Lacombe and Y. De Conchy

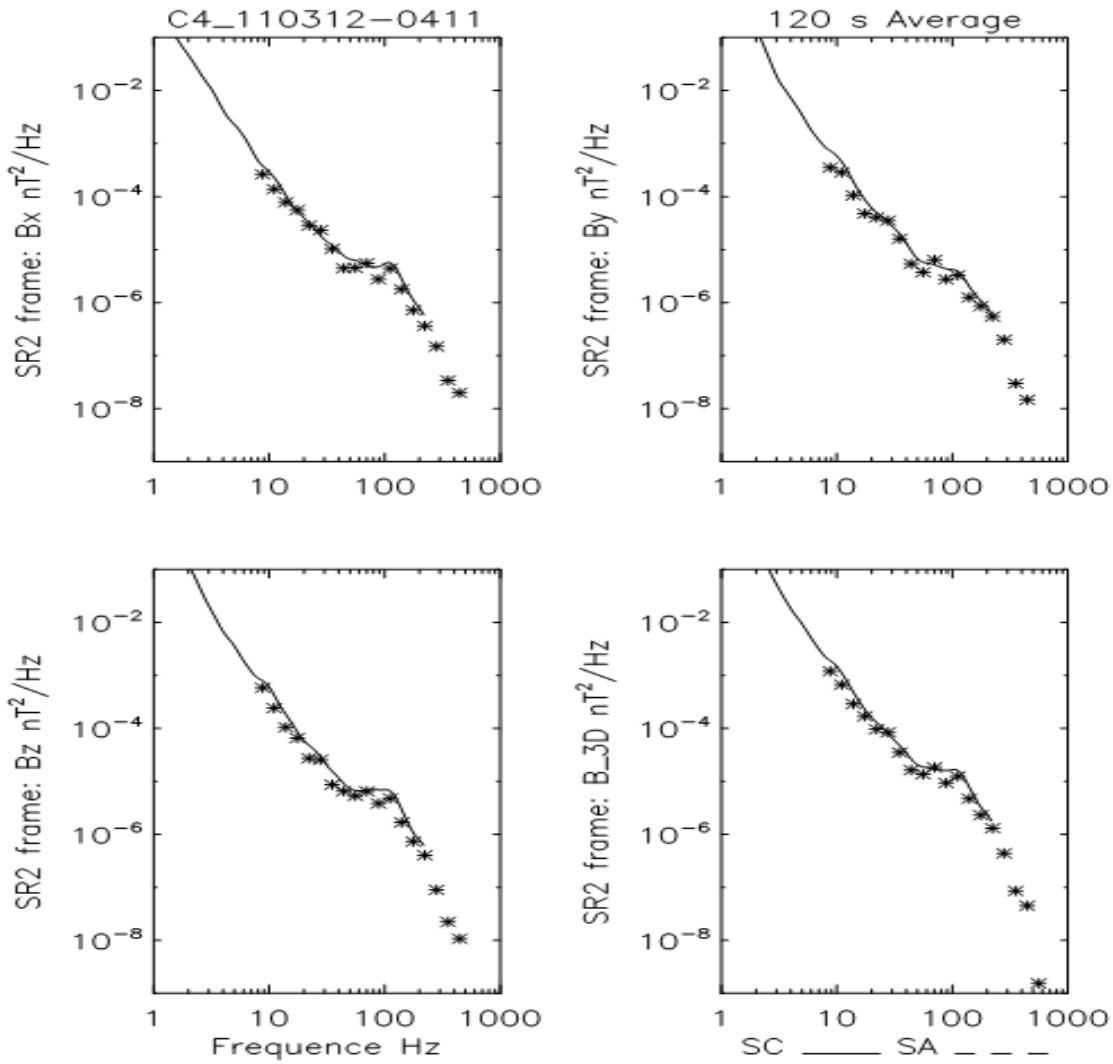

Figure 30: Same as Figure 29 for SC4

7.7 Continuity between FGM, STAFF–SC and STAFF–SA

Figure 31 below shows a combination of FGM, STAFF-SC and SA data for magnetic and STAFF-SA and EFW for electric components. A good continuity is observed between the data sets, acquired during a magnetopause crossing, with a rather constant slope until 200 Hz. Small discrepancies between STAFF-SC and STAFF-SA has been corrected since this work. The STAFF sensitivity is also plotted.

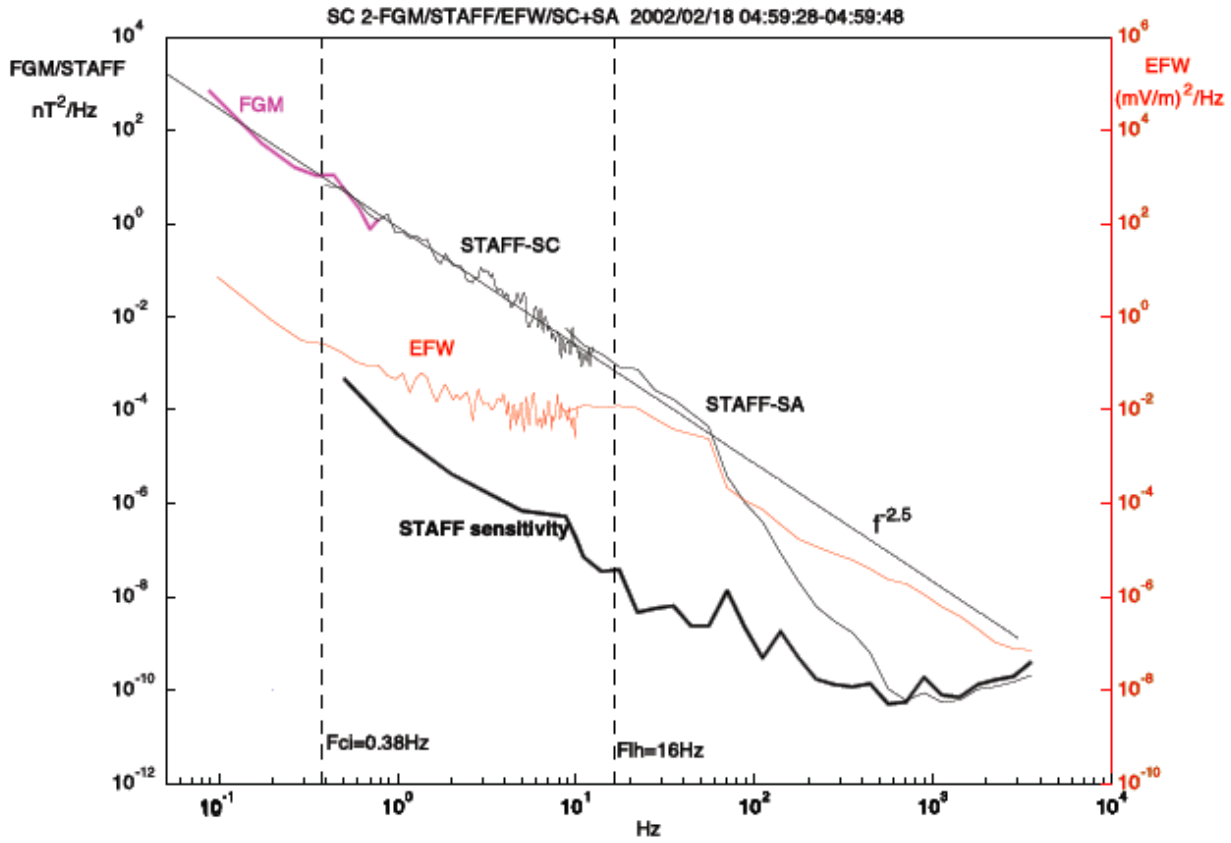

Figure 31: Combination of FM, STAFF-SC and SA spectra

7.8 Statistical comparisons between STAFF–SC and STAFF–SA

For these comparisons, data from several periods have been used to widely cover the possible magnetic fluctuation intensities range. The intervals are:

- 16/12/2001 from 05:30 to 06:30 (high intensity fluctuations in the magnetosheath).
- 19/12/2001 from 02:40 to 03:40 (low intensity fluctuations in the magnetosheath).
- 03/02/2001 from 17:00 to 18:00 (very low intensity fluctuations in the solar wind).
- 19/02/2002 from 01:00 to 02:00 (low intensity fluctuations in the solar wind).

For each of these intervals, the data have been divided into 20 seconds length sub-intervals. On each of those sub-intervals, the average values have been computed around 8.8 Hz for both the STAFF-SA (SA) and the STAFF-SC (SC) fluctuations. These average values are called respectively <*sa*> and <*sc*>. Practically, the following procedure has been used:

For SA, the time resolution of each channel is one second. Therefore, <*sa*> is the average of the 20 consecutive spectral values at the first SA frequency channel, that is at 8.8 Hz. As indicated previously, the 27 SA frequency channels are distributed logarithmically in the frequency range between 8 Hz to 4 kHz. Each of these 27 channels measures fluctuations in a band Δf around a central frequency f_0 with $\Delta f/f_0 \approx 0.26$. Therefore, for the first SA frequency channel,

the fluctuations are recorded over the frequency range ~7.6 to ~9.9 Hz. For SC, the PSDs spectra of the whole waveform signal are first computed on each 20 seconds sub-interval. Then, <*sc*> is the average PSD in the frequency band ~7.6 to ~9.9 Hz.

In the figures below, for each of the three components, for Cluster 1 and for all the 20 seconds subintervals, <*sc*> is plotted as a function of <*sa*>. On these figures the magnetic fluctuations are displayed in nT_2/Hz. The diamonds represent the magnetosheath high intensity fluctuations, the stars represent the magnetosheath low intensity and the crosses represent the solar wind data. Note that the plots and the following conclusions are very similar for all the other Cluster spacecrafts. Two main conclusions arise from this study:

- Globally the agreement between <*sc*> and <*sa*> is good while the fluctuations intensity is larger than $\sim 10^5\ nT^2/Hz$ (diamonds). For intensities lower than this threshold (stars), there is no agreement. Only an extensive physically based study would provide us the fluctuations absolute level to determine which experiment (SC or SA).gives the true measurement. Note that this threshold value ($10^5\ nT^2/Hz$) is close to the search coils (SC) sensitivity level at this frequency ($10^6\ nT^2/Hz$).

- For all spacecraft, the agreement is better on the Z-component fluctuations than on the X and Y. It is probably due to the despin procedures applied to both SA and SC. For SA, the pairs of spin-plane magnetic field components are despun aboard the spacecraft. For SC, the despin is performed on the ground. For SC the despin procedure has noticeable effects on the X and Y components around the spin frequency (0.25 Hz) and almost no effects on the Z component.

In summary, the agreement between STAFF-SA and STAFF-SC is good, while the magnetic fluctuation level around 8.8 Hz is larger than 10^{-5} nT^2/Hz. Consequently, the magnetic PSD data around this frequency, with values smaller than this threshold should be used with caution.

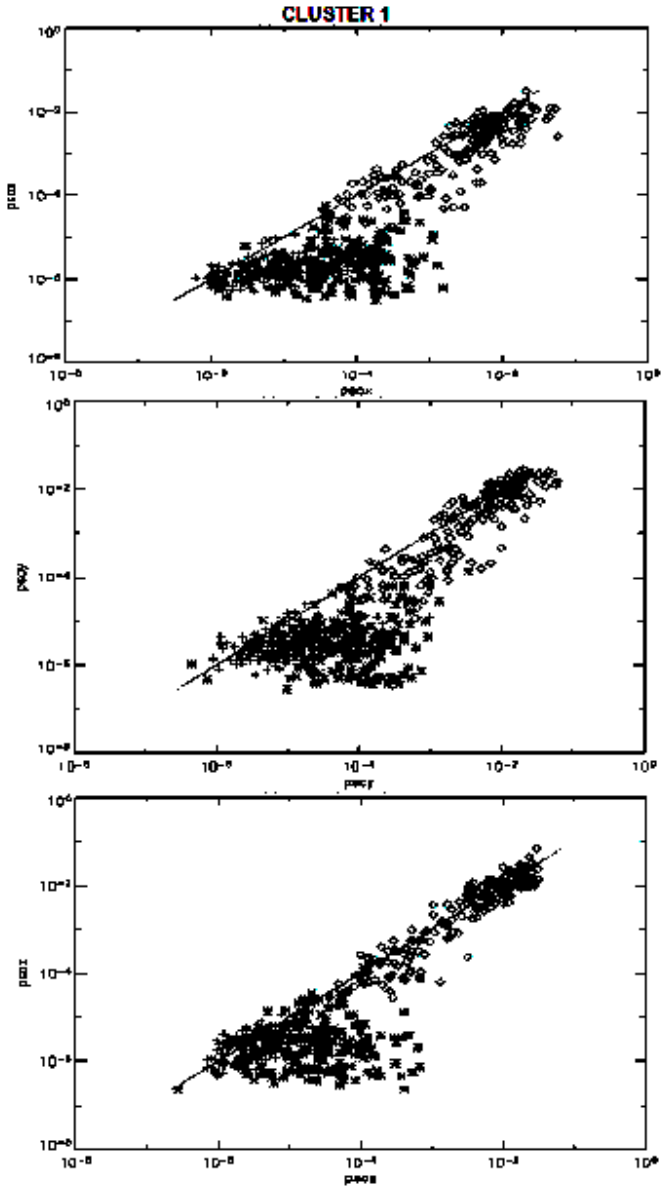

Figure 32: Comparison of magnetic fluctuations levels between SC and SA at 8.8 Hz, for low and high intensity values

7.9 Comparison of STAFF–SA with other WEC instrument

Here are presented cross-calibration results between STAFF and other WEC instruments, first comparisons of magnetic fluctuations between STAFF-SA and WBD, then between STAFF-SA electric field fluctuations and EFW, WHISPER and WBD. Since the comparisons between STAFF-SA and WBD have been done on a reduced data set, they are probably not fully representative and further comparisons should be done.

7.9.1 Magnetic fluctuations comparisons between STAFF-SA and WBD

This comparison is done first on a specific event. A chorus type event detected when WBD and STAFF-SA were both operating has been chosen (see below Figure 33)

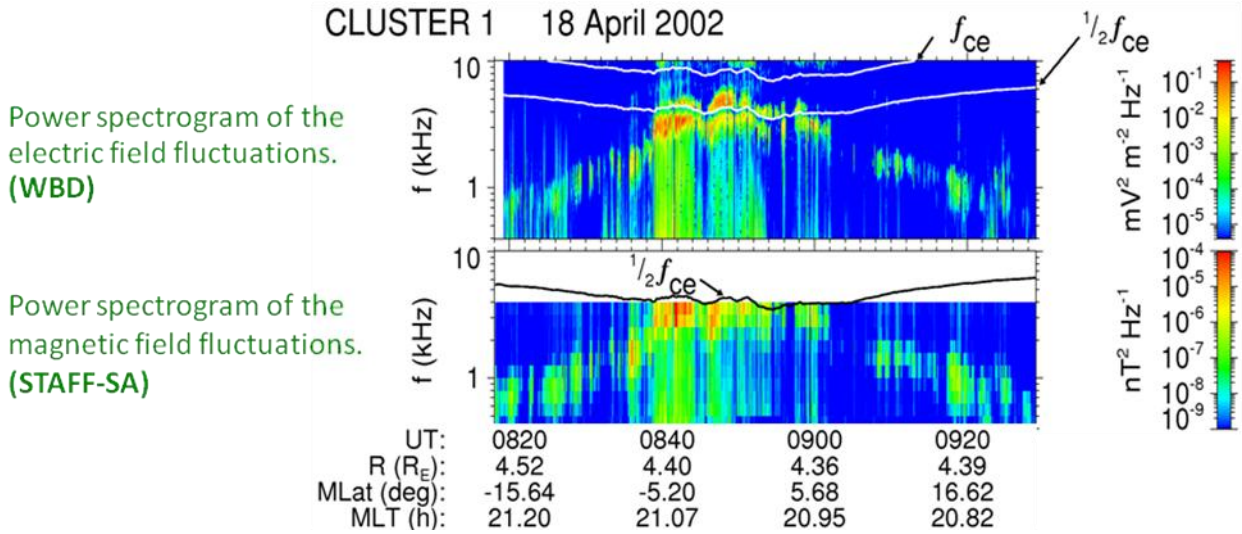

Figure 33: event chosen for comparing STAFF-SA and WBD

The analysis has been done during the most intense part of the event, between 08:44:55 and 08:53:48. The WBD magnetic spinning component By is acquired 10 s over 50 s of data (covering periods where Whisper is active). A FFT is applied to the time series samples corresponding to the 4 s STAFF-SA analysis intervals and the power is averaged over frequency intervals corresponding to the 27 STAFF-SA frequency bins. The STAFF-SA data are despun and analyzed onboard. Figure 34 shows the results of the comparison, for the whole frequency range and for the 3 STAFF-SA bandwidths.
The best fit is for C band (500-4000 Hz), which corresponds to the frequency range of the maximum wave power (see Figure 34).

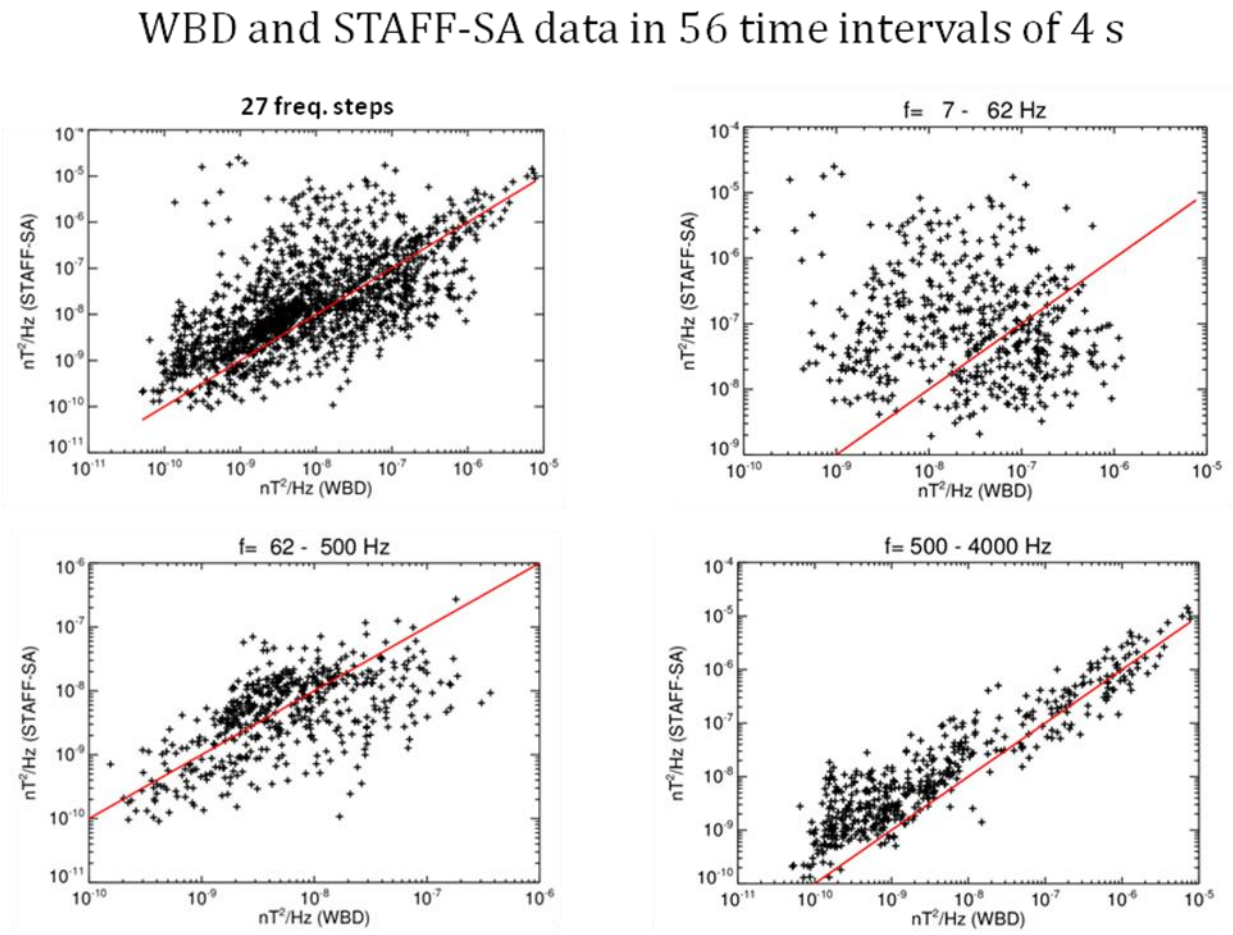

Figure 34: comparison of STAFF-SA and WBD power density of magnetic fluctuations (in nT2/Hz) for the whole frequency range (top-left) and for the different STAFF-SA frequency bands A, B, C.

The median power ratio (STAFF-SA/WBD) is shown in Figure 35. For strong waves the ration is about 4 in C band, about 1 for low amplitude waves (B band). The behavior in A band, where the signal is at noise level, seems to be linked to the WBD high pass filter.

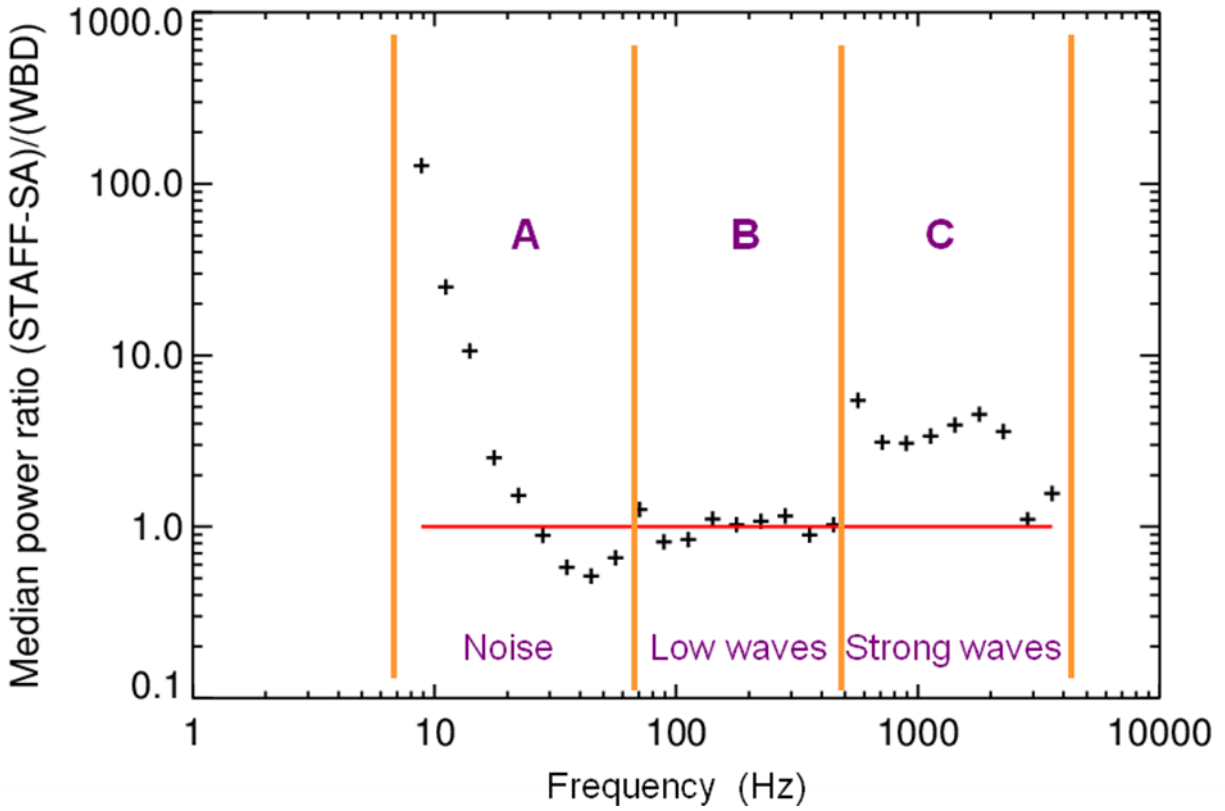

Figure 35: Plot of the median power ratio between STAFF-SA and WBD power calculated in frequency bins similar to those of STAFF-SA and calculated over similar time periods

For the lower frequency band A in which there was no wave signal for the studied event, one sees the effect of the WBD high pass filter.

The above differences between the two experiments can be partly explained by the differences in the data acquisition and processing. The behavior of the background noise is explained by the WBD high pass filter. The different between band B and C is still to be understood. For the higher signal, the ratio of 4 in power (then 2 in amplitude), should be corrected with the revised transfer functions to be applied on the different on board analysers.

7.9.2 Electric fluctuations comparisons between STAFF–SA and EFW

For these comparisons, we have used data of two different periods, one when the spacecraft were in normal bit rate and one in high bit rate. This allows to make the comparison for two different frequency ranges, around 8 Hz and around 70 Hz.
The first period, in NBR, is for the period 16/03/2002 from 05:00 to 08:00, which corresponds to a cusp traversal. The EFW waveforms have been retrieved using the ISDAT software. For this period, data (using the P1234 parameter on ISDAT) were available only for Cluster 3 & 4.

For the SA/EFW comparison, the analysis procedure approach used for magnetic component and described in the previous section has been adopted for the electric component. On the two next Figures, for each of the two electric components, for Cluster 3 and for all the 20 seconds sub-intervals the SA electric fluctuations have been plotted as a function of the EFW ones in the range 7.6 to 9.9 Hz.

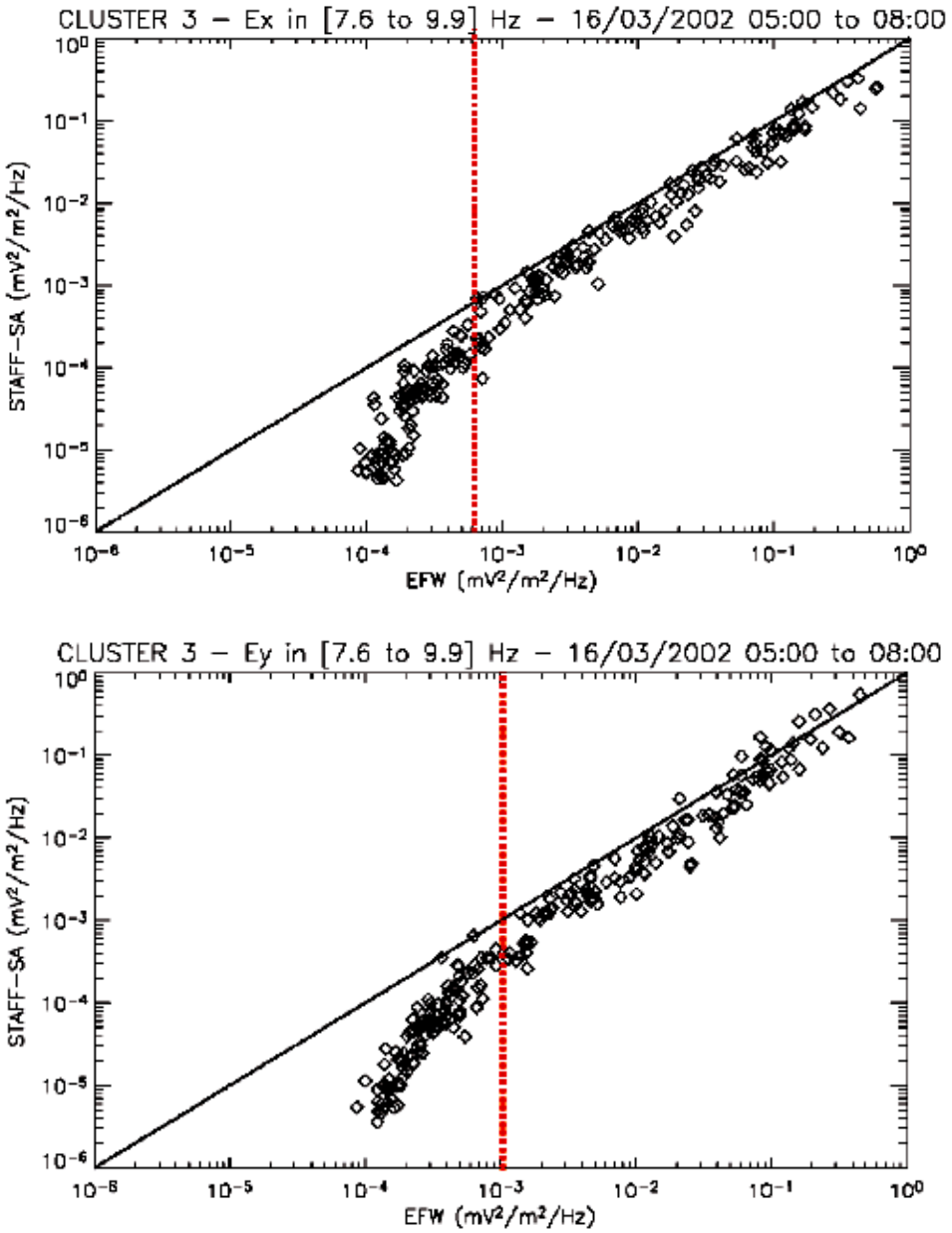

Figure 36: Comparison between STAFF-SA and EFW of electric field power at frequency ~ 8.8 Hz in NBR mode for the Ex (top) and Ey component (bottom)

For the second period, in HBR, the results plotted in Figure 37 correspond to an hour of data for S/C2 on 19 April 2001.

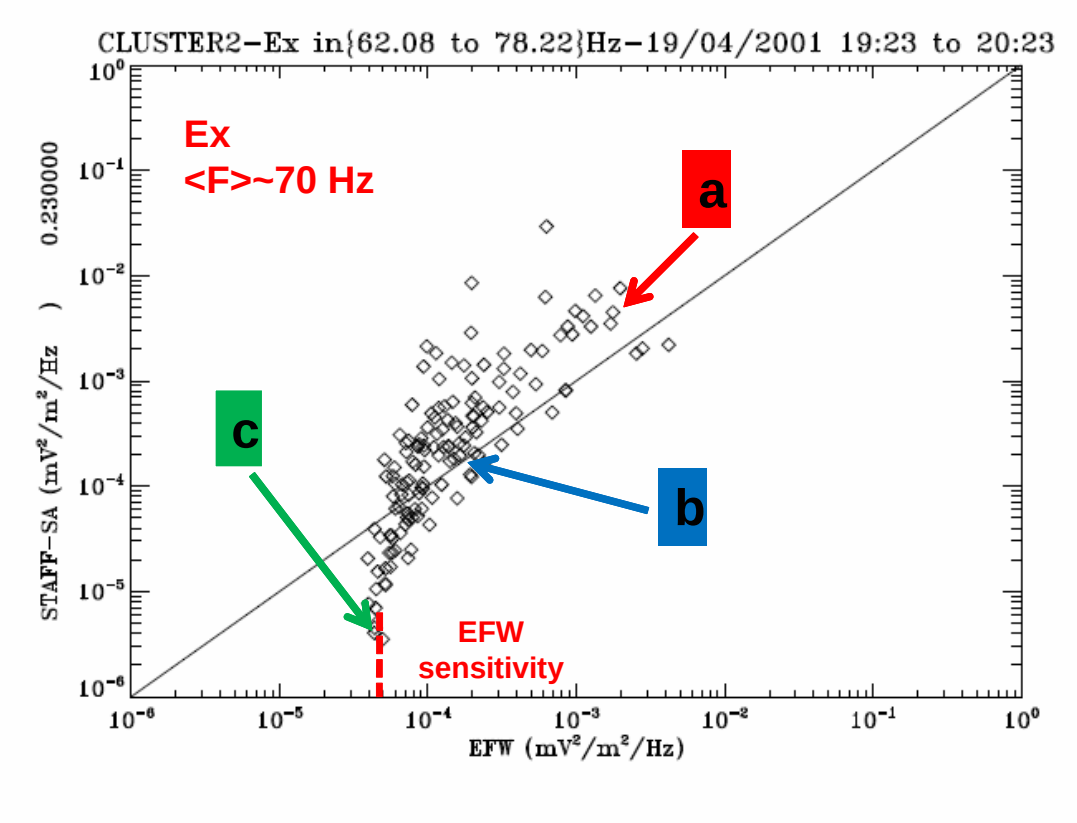

Figure 37: Comparison between STAFF and EFW electric components in HBR mode

On these three figures the electric fluctuations are displayed in $(mV/m)^2/Hz$. The data are globally in good agreement when the intensity of the fluctuations is larger than a given threshold. For the four spacecraft, this threshold is about $10^{-3}(mV/m)^2/Hz$ around 8 Hz and 10^{-4} $(mV/m)^2/Hz$ around 70 Hz. Below these threshold, the two experiments disagree. It is probably due to the EFW experiments sensitivity level which reaches those value at these frequencies [A. Ericksson, private communication].

***Conclusion of comparisons between STAFF-SA and EFW*:** the agreement is good while the electric fluctuations level around 8.8 Hz is larger than *6 to 10 x 10^{-4} $(mV/m)^2/Hz$*. As this latter value is known to be close to the EFW experiment sensitivity, the electric PSD data, around this frequency, should be retrieved preferentially from the STAFF-SA experiment. In the same way, in high bit rate if the fluctuation level around 70 Hz is below *6 to 10 x 10^{-5} $(mV/m)^2/Hz$*, one should preferably use SA data.

7.9.3 Electric fluctuations comparisons between STAFF–SA , WHISPER and WBD

A first comparison between those three instruments measurements is given in Figure 38. On this figure are displayed electric field fluctuations measured at the same time by STAFF-SA, WHISPER and WBD. For WHISPER, the data are retrieved with ISDAT with the calibration files updated on 2001-02-28 and named C1234_CT_WHI_20010504_V002.cal. The selected parameter is “WHISPER NATURAL” For WBD the PSDs were provided by Jolene Pickett and

Ondrej Santolik, using the calibration coefficients produced by Rich Huff on 09 July 2001. Depending on the frequency overlaps, the agreement is more or less good between the three experiments.

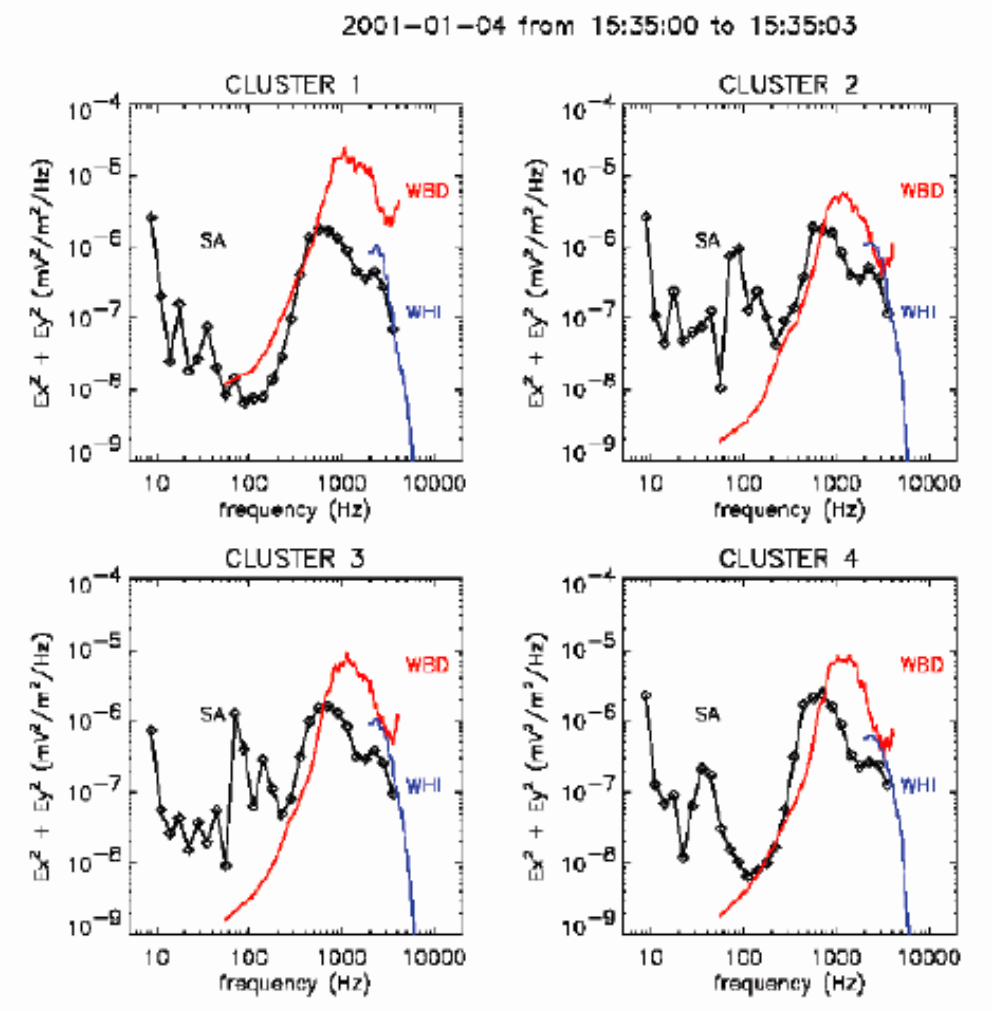

Figure 38: a first comparison between results from the STAFF-SA, Whisper and WBD instruments on a single event for the 4 spacecraft. Significant discrepancies are observed

Whereas there seems to be good agreement between Whisper and WBD (except on S/C 1), the WBD/STAFF comparison shows discrepancies to be solved. The understanding of these significant differences will have to take into account the differences between these instruments in collecting their data.

A final comparison is done using STAFF-SA and Whisper data, obtained on a longer time interval

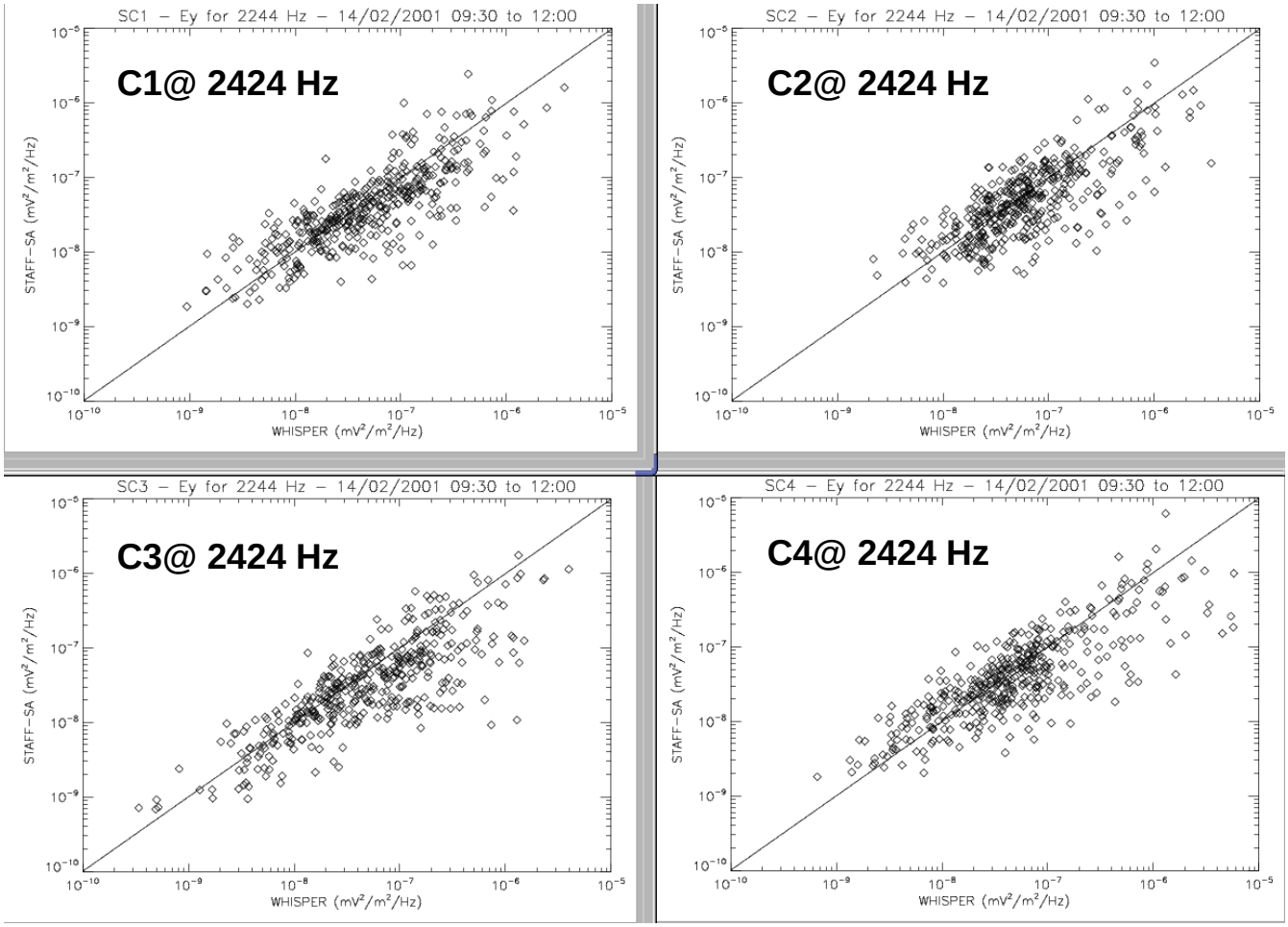

Figure 39: Comparison between STAFF-SA and Whisper (medium intensity)

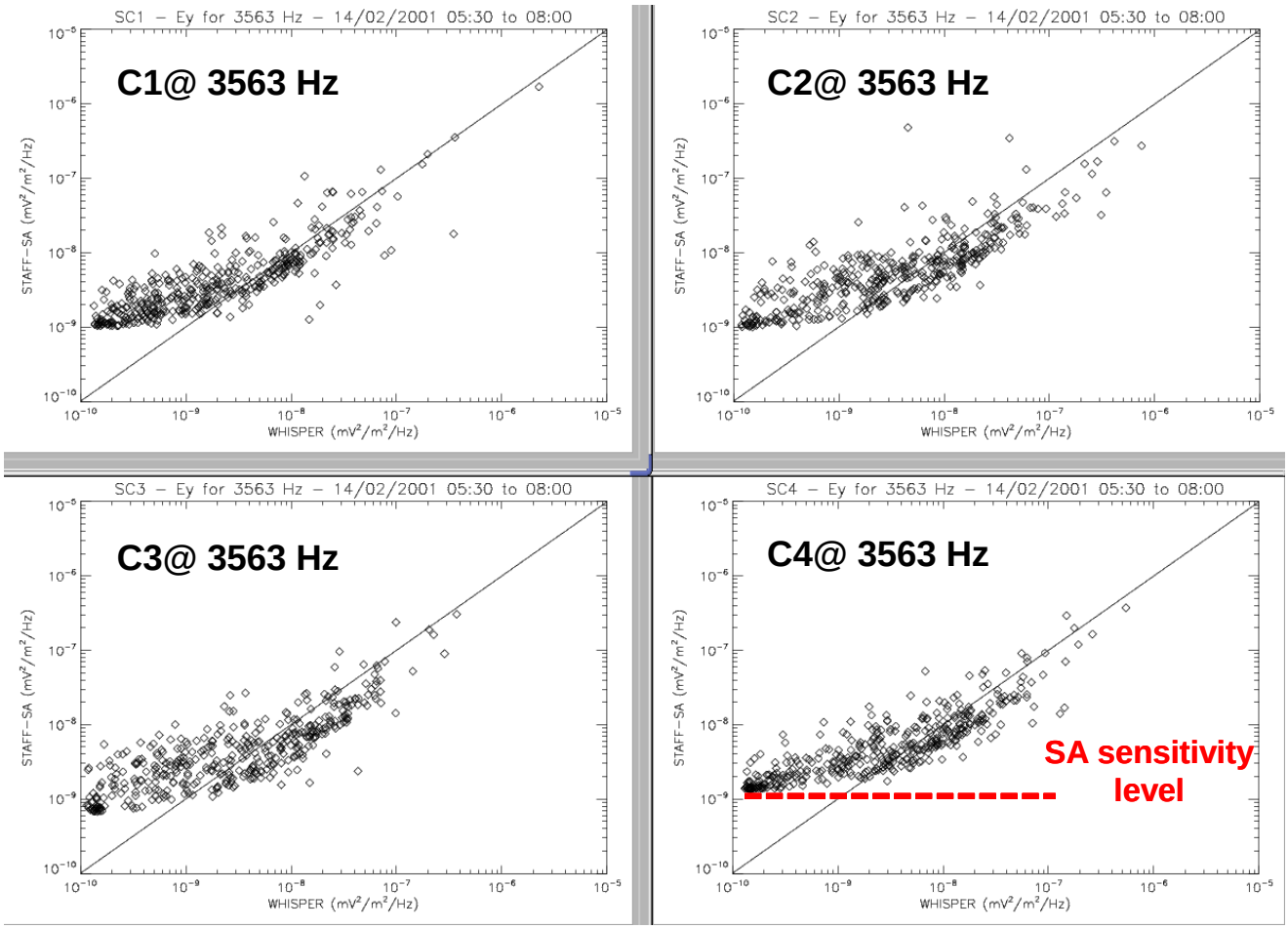

Figure 40: Comparison between STAFF-SA and Whisper (low intensity)

l

This comparison is done on 2 different frequencies channels and different regions. Figure 39 displays data collected close to the magnetopause with medium wave intensities, while Figure 40 shows data collected in the plasmathrough with lower level intensities. The agreement between the 2 instruments is rather good on the first example, and presents a significant difference for the lower level intensities, which can be attributed to reaching the sensitivity level for STAFF-SA.

In conclusion, the agreement between SA and WHISPER is quite good. Nevertheless, at high frequency (around 3 500 Hz) the sensitivity level of STAFF-SA, not as good as the Whisper one, is evidenced.

8. Summary

The calibrations and cross-calibrations results presented here illustrate the improvements obtained between the initial STAFF products delivered to the CAA and the data which are available today, obtained with the latest calibration functions.
In particular the significant discrepancies found for STAFF-SC between SC1 and the other spacecraft and between STAFF-SC and FGM has been well understood and corrected, the residual differences (less than 1% in intensity and 3° in phase) being more than satisfactory.

The previous calibration error on S/C1 has no influence on the other instruments using STAFF magnetic search coil, as it affected only frequencies below 8 Hz.
Although some coherence has been evidence between the wave instruments collecting data in the overlapping frequency range (STAFF, EFW, Whisper, WBD), significant discrepancies have been found, depending on the frequency and the waves intensity. Hence, the users shall pay attention to the differences identified so far, particularly when data are analyzed close the instruments respective sensitivity levels. Efforts are on going to understand better these discrepancies, taking into account, in particular, the different modes of operations and data collections

9. References

[1] Nicole Cornilleau-Wehrlin ; Chauveau, P.; Louis, S.; Meyer, A.; Nappa, J. M.; Perraut S.; Rezeau, L.; Robert, P.; Roux, A. and C. De Villedary: **The cluster spatiotemporal analysis of field fluctuations (STAFF) experiment**. *Space Science Review* **79**: 107- 136, 1997.

[2] N. Cornilleau-Wehrlin, C. Burlaud, **"User Guide to the STAFF measurements in the Cluster Active Archive (CAA)",** ESA CAA-EST-UG-001.

[3] P. Robert, **« Les procédures Roproc pour le traitement des données de CLUSTER/STAFFSC, FGM et ORBITE »,** Version 2.0, Rapport interne CETP, septembre 2003.
ftp://ftp.lpp.polytechnique.fr/robert/keep/Transfert/Roproc_V2p0.pdf

[4] P. Robert, **"Roproc Command Language, a set of linked commands for spatial data processing",** Version 02, CETP Internal report, Novembre 2004.
ftp://ftp.lpp.polytechnique.fr/robert/keep/Transfert/RCL_V2.pdf

[5] P. Robert, **"Wave Calibration methods for nolinear frequency transfer function"**, DRAFT, version 1.1, May 11 2007, CETP Internal report to be finished.

[6] P. Robert, **"ROCOTLIB: a Coordinate Transformation Library for SolarTerrestrial studies"**, version 1.8, update of CETP Internal report n° RI-CETP/01/2003, Novembre 2003.
ftp://ftp.lpp.polytechnique.fr/robert/keep/Transfert/ROCOTLIB%20v1.8u.pdf

[7] C. C. Harvey, Belkacemi, M., Manning, R., Wouters, F., de Conchy, Y.: **STAFF Spectrum Analyzer, Conversion of the Science Data to Physical Units.** Technical Report OBSPM-N-0001, issue 7, rev. 5, Observatoire de Paris Meudon.

[8] Santolik O., **"Propagation Analysis of STAFFSA Data with Coherency Tests (A User's Guide to PRASSADCO)",** LPCE/NTS/073.D, Lab. Phys. Chimie Environ./CNRS, Orleans, France, 2003. (http://os.matfyz.cz/PRASSADCO/guide.pdf).

[9] K. Nykyri, B. Grison, **P. J. Cargill**, B. Lavraud, E. Lucek, I. Dandouras, A. Balogh, N. Cornilleau-Wehrlin, and H. Reme **Turbulence study in the highaltitude cusp: Cluster FGM and STAFF observations**, Ann Geophys., 24, 1057-1075, 2006.

[10] Milan Maksimovic and the STAFF Team, **"Cluster Cross-Calibration Workshop",** ESTEC 02/May/2006.

[11] All minutes of cross calibration workshops are available on the CAA web site, at
ftp://ftp.rssd.esa.int/pub/Cluster/MoM/CAA/CrossCalibration/

[12] P. Robert, N. Cornilleau-Wehrlin, R. Piberne, Y. de Conchy, C. Lacombe, V. Bouzid, B. Grison, D. Alison, and P. Canu**: CLUSTER STAFF search coils magnetometer calibration – comparisons with FGM**, GID, 3, 679–751, 2013.

10. Appendix A: Coordinate systems used by STAFF definitions

To transform telemetry data into significant physical units we need to convert the data from the sensor coordinate system into one or another system, and in particular to transform from the spinning system into a fixed one, with respect to Sun and Earth for instance. The following sections are dedicated to define all intermediate coordinate systems required for this operation. Notice than these definitions can be used for other experiment of the same type, one any other mission.
All transformation matrixes are named as: A_to_B where A and B are two different coordinate systems. To convert a vector given in the A system to the same vector expressed in the B system, the following expression is used:

$$\begin{pmatrix} x \\ y \\ y \end{pmatrix}_B = A\_to\_B \begin{pmatrix} x \\ y \\ y \end{pmatrix}_A$$

For general computation of this kind of matrix, see [8, Robert, 2003].

10.2 The Sensor Coordinate System (SCS)

This is the system where the original signal is measured (see Figure 41 below). This system could be a non perfect orthogonal system.

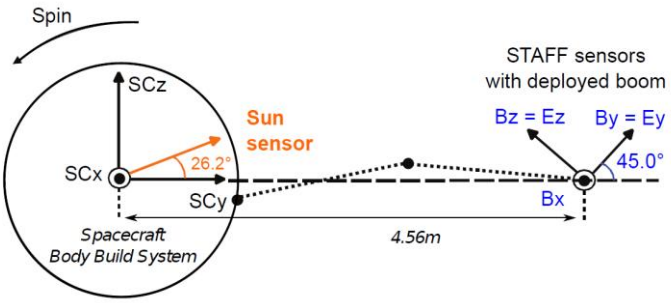

Figure 41 : Position des antennes de STAFF dans le repère « Body Build » lié au satellite.

10.3 The Orthogonal Sensor System (OSS)

This is a Cartesian orthogonal coordinate system. The original sensor system can be a non orthogonal system, the first step is to transform the data vector in an orthogonal coordinate system: Z axis being the reference of the new Orthogonal Sensor System. The corresponding matrix, called “SCS_to_OSS”, close to a unit matrix, is required and must be applied: values are supposed to be constant in time. Nevertheless, in a first time, taking into account the low deviation of the sensor to an orthogonal system for CLUSTER/STAFF (~0.2°), this correction is not applied and the matrix is set to unity matrix.

$$SCS\_to\_OSS \cong \begin{pmatrix} 1 & 0 & 0 \\ 0 & 1 & 0 \\ 0 & 0 & 1 \end{pmatrix}$$

If the user wants to do this correction, he can use the formulas given in section 9.6.1 which allows the transformation from a non orthogonal system to an orthogonal one.

10.4 The Data Sensor System (DSS)

The Body Build System (BBS, see next section) is a system fixed to the geometry of the spacecraft, and is used as the spacecraft system reference for all the experiments. Generally, for most of spacecraft missions, the Z axis is close to the maximum principal inertia axis also called the spin axis (for spin stabilized spacecraft). Nevertheless, for CLUSTER, this axis has been defined as the X axis (see Fig. 14).
In all our data, the convention taken is Z=spin axis. It means that we have an intermediate coordinate system, called Data Sensor System (DSS) which corresponds to the previous OSS, but where the axes are permuted, to make Z close to the spin axis.
By respect to the Fig. 1, X_{OSS}, Y_{OSS}, Z_{OSS}, becomes Y, Z, X in DSS.
This permutation is obtained by the following matrix:

$$OSS\_to\_DSS = \begin{pmatrix} 0 & 1 & 0 \\ 0 & 0 & 1 \\ 1 & 0 & 0 \end{pmatrix}$$

10.5 The Body Build System (BBS)

In the case of CLUSTER, the Z axis of the Data Sensor System is close to the X axis of the BBS system, but the misalignment angle is not easy to determine. It is also true for the small angle between this X_{BBS} and the true spin axis (precession and nutation motions). Nevertheless, an estimate of the cumulative angle is done in next subsection. Here, we neglect this small misalignment and assume $Z_{DSS} = X_{BBS}$. In all cases, 2 other axis may be rotated by an important angle (see Fig. 1). The corresponding matrix is required, called "DSS_to_BBS": values are supposed to be constant. Practically, for the STAFF search coils of CLUSTER, this matrix is a rotation matrix of $\alpha = 45°$.

$$DSS\_to\_BBS = \begin{pmatrix} 0 & 0 & 1 \\ \cos\alpha & -\sin\alpha & 0 \\ \sin\alpha & \cos\alpha & 0 \end{pmatrix}$$

10.6 The Spin Reference System (SRS)

The Spin reference system has its Z axis parallel to the spin axis. This is a spinning system, rotating at the spin frequency. As mentioned above, there is a small misalignment between the X_{BBS} axis and the Z_{SCS} axis, as there is another slight misalignment between the X_{BBS} axis and the Z_{DSS} axis (see Figure 42).

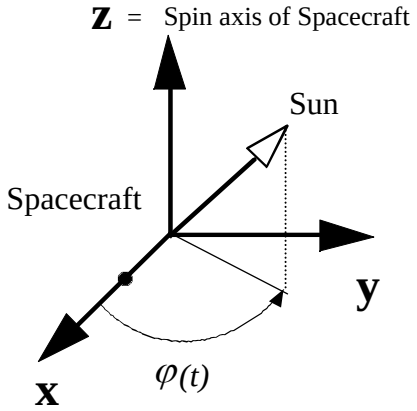

This is a spinning local system close to the measurement antenna of a spacecraft.

The Z-axis is the spin axis of the spacecraft.

The X-axis and Y-axis are perpendicular to the spin axis, and rotate at the spin frequency of the spacecraft.

The definition of the SR system need the knowledge of the spin axis in a fixed frame of reference as the GEI inertial system, and the value of the spin phase φ at a given time.

Figure 42: Definition of SR system

This is not easy to separate the two previous angles, but it is possible to estimate the small angle between the Z_{SCS} axis and the true spin axis which define Z_{SRS}. This angle θ could be estimated by the measurement of the low spin signal on the Z_{SCS} component (see section 9.5). If B_{xs}, B_{ys}, B_{zs}, are the amplitudes in nT of the spin sine on the 3 x, y, z components of the SCS system, this angle is estimated by :

$$\sin\tilde{\theta} = \frac{B_{zs}\sqrt{2}}{\sqrt{B_{xs}^2 + B_{ys}^2 + B_{zs}^2}}$$

This angle could be constant, but can have also small variations during operations on the spacecraft (trajectory modifications, etc.). It has been estimated to an average value of ~0.5°, and, in a first time, has not been taken into account. So, the "BBS_to_SRS" matrix is a simple circular permutation set to:

$$BBS\_to\_SRS \cong \begin{pmatrix} 0 & 1 & 0 \\ 0 & 0 & 1 \\ 1 & 0 & 0 \end{pmatrix}$$

10.7 The spin reference2 system (SR2)

The SR2 system, also called "SSS" for Spacecraft-SUN System, or "DS" for despun, is derived from the SRS system by a *despin* operation. The spinning Spacecraft is "stopped" just at the time where the X axis is in the plane containing the Z spin axis and the direction of the Sun. The rotation angle required is derived from the Sun pulse or any other quantity to compute the spin phase angle φ_s (see Figure 43).

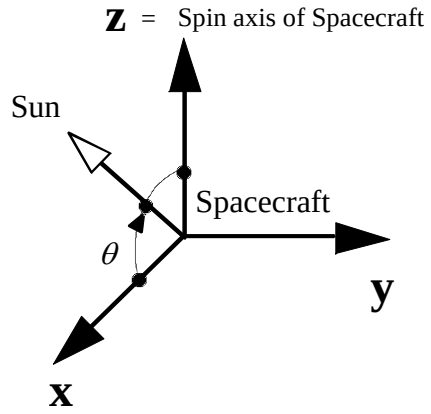

This is a fixed system useful for the spacecraft data processing. It is also called SCS, as "Spacecraft-Sun system", or DS system (Despun Satellite).

The Z-axis is the spin axis of the spacecraft.
The X-Z plane contains the direction of the Sun.

The X-axis is towards the day side.
The Y-axis is perpendicular to the spacecraft-Sun line.

The SR2 system rotates with the same period than the orbital period of the spacecraft with respect to the inertial system, while the declination θ varies continuously.

Figure 43: Definition of SR2 system (Despun)

This spin phase angle φ_s, and the corresponding time measurement, is required to build the "SRS_to_SR2" matrix. Terms of this matrix are fast varying with time. The phase angle φ_s is calculated for each time tag of the data thanks to the sun pulse signal. This gives, where f_s is the spin frequency:

$$SRS\_to\_SR2 = \begin{pmatrix} \sin(2\pi f_s t + \varphi_s) & \cos(2\pi f_s t + \varphi_s) & 0 \\ \cos(2\pi f_s t + \varphi_s) & -\sin(2\pi f_s t + \varphi_s) & 0 \\ 0 & 0 & 1 \end{pmatrix}$$

10.8 The Inverse SR2 system (ISR2)

This is equivalent to the SR2 system (or SSS) where the Z and Y axis has inverse sign. This system is useful for CLUSTER, where the Z axis of ISR2 system is close to the Z axis of the GSE system, so ISR2 is a rather good approximation of the GSE system, and does not requires knowledge of spin direction in GSE system.

$$SR2\_to\_ISR2 = \begin{pmatrix} 1 & 0 & 0 \\ 0 & -1 & 0 \\ 0 & 0 & -1 \end{pmatrix}$$

10.9 Simplification of the cumulative matrix products

Cumulative matrix product requested to transform original data given in SCS coordinate to a fixed coordinate system such as SR2 can be strongly simplified if we neglect all small misalignment angles mentioned above. By the way, the first mass processing on the STAFF-SC data was to produce a data base for the level 1 data (telemetry data) in the DSS system, which is delivered to the CSA. The only difference between the DSS with the SCS sensor coordinate is a circular permutation of the components to get the Z axis close to the spin axis, since we assume that the SCS is orthogonal and equal to the OSS (see section 8.4.2).
So to transform data expressed in DSS into the "fixed" SR2 we have to apply the cumulative matrix product:

$$\begin{pmatrix} x \\ y \\ y \end{pmatrix}_{SR2} = [SRS\_to\_SR2][BBS\_to\_SRS][DSS\_to\_BBS]\begin{pmatrix} x \\ y \\ y \end{pmatrix}_{DSS}$$

Assuming all small misalignment angles close to zero, we get:

$$[BBS\_to\_SRS][DSS\_to\_BBS] = \begin{pmatrix} \cos\alpha & -\sin\alpha & 1 \\ \sin\alpha & \cos\alpha & 0 \\ 0 & 0 & 0 \end{pmatrix}$$

Using expression of SRS_to_SR2 given in section 5.6, with $\omega_s = 2\pi f_s$ after some calculus we get:

$$\begin{pmatrix} x \\ y \\ z \end{pmatrix}_{SR2} = \begin{pmatrix} \sin(\omega_s t + \varphi_s + \alpha) & \cos(\omega_s t + \varphi_s + \alpha) & 1 \\ \cos(\omega_s t + \varphi_s + \alpha) & -\sin(\omega_s t + \varphi_s + \alpha) & 0 \\ 0 & 0 & 0 \end{pmatrix}\begin{pmatrix} x \\ y \\ z \end{pmatrix}_{DSS}$$

By neglecting all the small misalignment angles, the transformation from the Data Sensor System to the fixed SR2 system is simply reduced to a rotation in the spin plane of the fast varying angle:

$$\psi = (\omega_s t + \varphi_s + \alpha).$$

This simplification is used for CLUSTER/STAFF calibration, but cannot be used for spacecraft or rocket having precession or nutation, or a non constant direction of the spin axis. In this case, the full computation must be done.

10.10 The Geocentric Equatorial Inertial system (GEI)

The GSE system is a well known system, with the Z axis perpendicular to the Ecliptic plane, and the X axis toward the Sun. To do the transformation of the SSS to the GSE, the direction of the spin axis in the GSE system is required. Due to the gyroscopic effect of a spinning spacecraft, the spin axis is ~constant in an inertial system, and so has a yearly variation in the GSE system, excepted during spacecraft operations (see Figure 44).

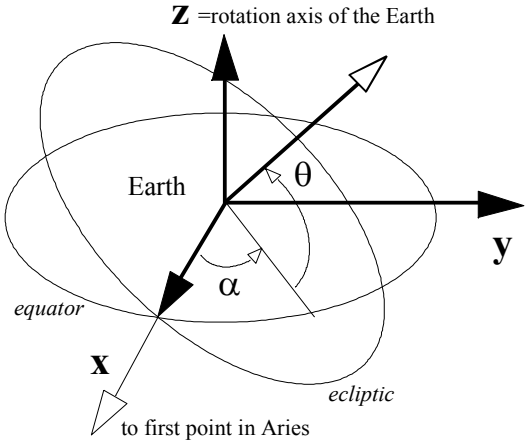

The Z-axis is parallel to the rotation axis of the Earth. The X-axis is defined by the intersection of the equator plane and the ecliptic plane, and is pointing towards the first point of Aries (Sun position at the vernal equinox). One can define the ***right ascension*** α *and the* ***declination*** θ *as:*

right ascension : $\alpha = \tan^{-1}(V_y/V_x)$

with α *in* $[\ 0°, 180°]$ *for* $V_y > 0$

α *in* $[180°, 360°]$ *for* $V_y < 0$

declination $\theta = \sin^{-1}(V_z/V)$

with θ *in* $[-90°, 90°]$

Figure 44 : Definition of GEI system:

SR2 to GSE transformation is done using module "tsr2gse" routine of ROCOTLIB software (see Robert, 1993, 2003, 2004). The Cartesian GSE coordinates of the direction of spin axis is required, as the corresponding time measurement. To transform spin right ascension and spin declination angle, given in STAFF-SC CSA data in Geocentric Equatorial Inertial system (GEI), routine "tgeigse" can be used. Those angles are also available in the auxiliary files available at CSA (latitude and longitude angles of the spin axis direction in GSE).

Note that in GSE system, each component mixes both parallel and perpendicular components to the spin axis. Because sensitivity is strongly different at low frequency on the parallel and perpendicular components in SR2 system, it is recommended to filter the date below ~0.6Hz before coordinate transformation. This is done for CSA Complex Spectra products.

10.11 The Geocentric Solar Ecliptic system (GSE)

Well known and very used system (see Figure 45).

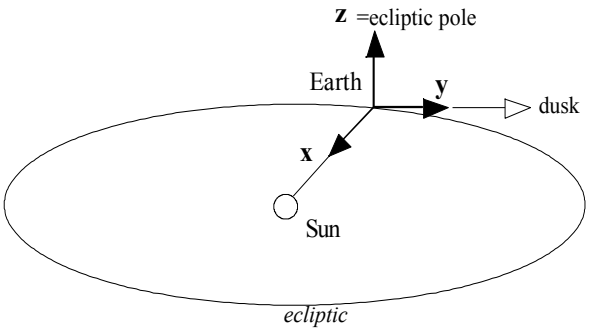

The X-axis is pointing from the Earth towards the Sun.

The X-axis and the Y-axis are included in the ecliptic plane.

The Y-axis is pointing toward the dusk, opposing to the planetary motion.

The Z-axis is parallel to the ecliptic pole. The GSE system has a yearly rotation with respect to the inertial system.

Figure 45: Definition of GSE system

10.12 Geocentric Solar Magnetospheric system (GSM)

This system is known in space physics to properly organize the data, insofar as it reconciles the direction of the sun and the plane of the Earth magnetic meridian (see Figure 46).

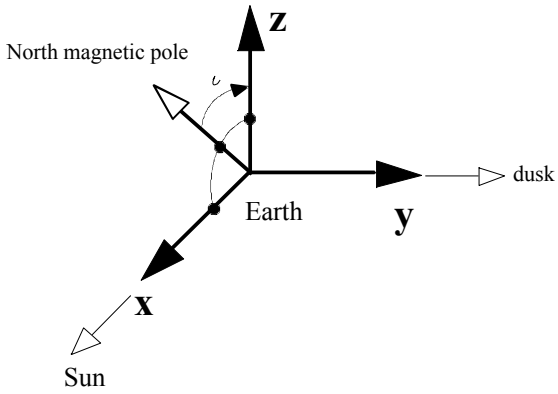

The X-axis is pointing from the Earth towards the Sun.

The X-Z plane contains the dipole axis.

The Y-axis is perpendicular to the Earth's magnetic dipole, towards the dusk and include in the magnetic equator plane.

Figure 46: Definition of GSM system

The positive Z-axis is chosen to be in the same sense as the northern magnetic pole: the dipole tilt angle ***i*** is positive when the north magnetic pole is tilted towards the Sun. In addition to a yearly period due to the motion of the Earth about the Sun, the GSM system rocks about the Solar direction with a 24 h period.

10.13 Magnetic Field Aligned system (MFA)

This system is essential to study the polarization of waves. Indeed, most of the plane waves are characterized by their direction of rotation around the magnetic field, and by the angle between the normal to the wave plane and the main field (see Figure 47). It has therefore been introduced for this purpose [16, Robert, 2000].

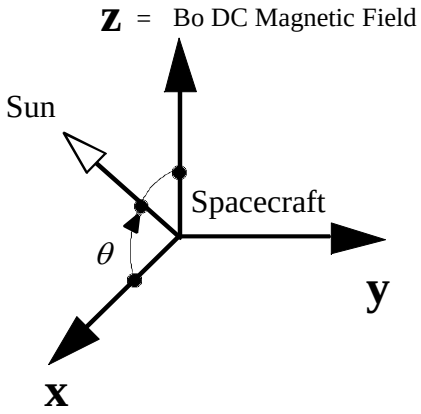

Figure 47: Definition of MFA system

This is a system useful for physic, but the meaning of the Bo DC magnetic field must be knew, as its time variation (see ref. [16]).
The Z-axis is the DC magnetic field vector.
The X-Z plane contains the direction of the Sun.

The X-axis is towards the day side.
The Y-axis is perpendicular to the spacecraft-Sun line.

The MFA system move continuously with the time variation of the DC magnetic field.